We are IntechOpen, the world's leading publisher of Open Access books Built by scientists, for scientists

4,800
Open access books available

122,000
International authors and editors

135M
Downloads

Our authors are among the

154
Countries delivered to

TOP 1%
most cited scientists

12.2%
Contributors from top 500 universities

CLARIVATE ANALYTICS BOOK CITATION INDEX INDEXED

WEB OF SCIENCE™

Selection of our books indexed in the Book Citation Index in Web of Science™ Core Collection (BKCI)

Interested in publishing with us?
Contact book.department@intechopen.com

Numbers displayed above are based on latest data collected.
For more information visit www.intechopen.com

Chapter 11

Fumarolic Minerals: An Overview of Active European Volcanoes

Tonči Balić-Žunić, Anna Garavelli,
Sveinn Peter Jakobsson, Kristjan Jonasson,
Athanasios Katerinopoulos,
Konstantinos Kyriakopoulos and
Pasquale Acquafredda

Additional information is available at the end of the chapter

http://dx.doi.org/10.5772/64129

Abstract

The fumarolic mineralogy of the Icelandic active volcanoes, the Tyrrhenian volcanic belt (Italy) and the Aegean active arc (Greece) is investigated, and literature data surveyed in order to define the characteristics of the European fumarolic systems. They show broad diversity of mineral associations, with Vesuvius and Vulcano being also among the world localities richest in mineral species. Volcanic systems, which show recession over a longer period, show fumarolic development from the high-temperature alkaline halide/sulphate, calcic sulphate or sulphidic parageneses, synchronous with or immediately following the eruptions, through medium-temperature ammonium minerals, metal chlorides, or fluoride associations to the late low-temperature paragenesis dominated by sulphur, gypsum, alunogen, and other hydrous sulphates. The situation can be different in the systems that are not recessing but show fluctuations in activity, illustrated by the example of Vulcano where the high-temperature association appears intermittently. A full survey of the mineral groups and species is given in respect to their importance and appearance in fumarolic associations.

Keywords: fumarolic minerals, Iceland fumaroles, Tyrrhenian volcanic belt fumaroles, Aegean active arc fumaroles, mineral sublimates

1. Introduction

At present, there are three active volcanic provinces in Europe (**Figure 1**). The first one is situated in NW corner, on the spreading Mid-Atlantic Ridge, nurtured by the Iceland hot spot and causing intermittent activation of numerous volcanoes. The second is the Tyrrhenian volcanic belt with a very active volcanism. It comprises the Roman comagmatic province, which is related to the extension of the Tyrrhenian basin and the rollback of the Apennine chain, and the Aeolian Arc, the genesis of which is generally ascribed to the subduction of the Ionian microplate under Calabria. The third one is the Aegean Active Volcanic Arc, related to the eastern Mediterranean lithosphere subduction under the Aegean-Anatolian microplate. It is characterized by a dormant or recessing volcanism. Is this remarkable variety in causes of volcanism and its activity reflected in the products of volcanic emanations, and in which way? This chapter tries to summarize the mineralogical evidence and give the answer to this question.

Figure 1. Europe from the space with locations of the three volcanic provinces described in this chapter.

There is no process in geology that, on closer inspection, can be called simple. Compared to the processes on the similar scale, the mineralization of a fumarole or a fumarolic field might well be the most complex one. It happens in an open system with high kinetic energy, high mass transport rate, and subject to constantly fluctuating conditions. It involves reactions of gases, fluids, and solids at the boundary between the atmosphere, volcanic gases, meteoric water, hydrothermal solutions, lava, and country rock. Minerals in fumaroles form either as direct sublimates due to changes in temperature or composition of gases, as accumulations of aerosols carried by gas, through gas-solid reactions either by the assimilation of gas components or by leaching of solid, through temperature-induced reactions (mineral reactions, phase transitions, dehydration), through the action of water or vapour (hydration or dissolution) or

by crystallization from solution. Inspection of the literature about fumaroles reveals that authors use the following two distinct attributions: sublimates and encrustations. The term sublimate is used for the minerals formed by deposition from gases, and encrustations are formed from fumarolic fluids, but the study reveals many inconsistencies. The reason is that the processes mentioned earlier happen simultaneously at the same place and are entangled. Moreover, most of the minerals can be formed through more than one process. Here, we will consider all minerals in fumaroles that are formed under whatsoever influence of volcanic gases as fumarolic minerals and avoid making classifications that would have too many exemptions and in many cases be misleading. Another question is the definition of a fumarole itself. In their work on Icelandic fumaroles, Jakobsson et al. [1] distinguished the following two types of fumarolic associations: volcanogenic, which are formed by short-lived, shallow-rooted thermal systems and characterized by no discharge of water and by encrustations that are primarily product of magmatic degassing; and solfataric hydrothermal systems, which are long-lived with a deep-rooted source and surface exposures of high-temperature hydrothermal activity with extensive water-rock interaction. We keep our choice of the European localities as close as possible to the former type (volcanogenic), although it, in the context broader than specific Icelandic conditions, becomes more arbitrary because the fumaroles of a quiescent volcano closely resemble solfataras in their process of formation and mineralogy. The fumaroles on the Solfatara crater, which gave the name to the second category, are not identical in all their characteristics to those encountered on Iceland and illustrate how difficult it is to draw a border line. We are aware that our choice of what to include and what to exclude among the European places with gas emanations can be disputed, but we think that it illustrates well all stages of surface pneumatic processes connected to volcanism from its birth to its old stage and the last breaths of a volcano.

Measured with geological scales, fumaroles are short-lived phenomena. They are a surface or close to the surface feature of a volcano and much more sensitive to weathering than surrounding lava. The formation and dissolution and erosion of fumarolic minerals are contemporary processes, and when the gas emanations ultimately stop, the mineral content in the vents of fumaroles disappears in a short time and just the roots of a fumarolic system can be found in a fossilized form. Besides high chemical reactivity and instability, the fumarolic minerals often appear in microcrystalline aggregates and in the mixtures of many phases. The methods of research therefore require specific approaches and strategies.

2. Methods

2.1. Sample collection and preparation

In this work, the samples from 12 European volcanoes and other fumarolic systems have been investigated (Krafla, Askja, Hekla, Fimmvörðuháls, Eldfell, Surtsey, Vulcano, Etna, Soussaki, Milos, Santorini, and Nisyros). The data for Campi Flegrei and Vesuvius, plus additional data for investigated volcanoes, have been taken from the literature.

The samples have been left to cool down at atmospheric conditions after extraction. The fragile samples were mounted in plastic boxes fixed to avoid the physical damage. The less sensitive ones or those that were extracted in crushed form were sealed in plastic bags. After separating the chosen parts under the microscope, the samples for the X-ray diffraction (XRD) were crushed in agate mortar, and the samples for the scanning electron microscope with energy-dispersive spectrometer (SEM-EDS) analyses were sputtered with a 30-nm-thick carbon film using an Edwards Auto 306 thermal evaporator. The fumarolic samples are mostly composed of intimate mixtures of several minerals with micrometer-sized crystals. Even the most painstaking separation work is many times not in stand to produce a pure one-phase sample for powder X-ray diffraction (PXRD), and hence, the separation of multiple seemingly different portions of a sample was almost always performed in order to get the best overview of the phase composition.

2.2. X-ray diffraction

PXRD is the method of choice for the identification of minerals, alone or in mixtures, and for the quantitative phase analysis. Essential for handling complex mixtures is a diffractometer with high resolution, and therefore, the D8ADVANCE Bruker-AXS powder diffractometer with the primary Ge_{111} monochromator and the LinxEye silicon strip detector in reflection geometry was used for the measurement of bulk samples (at the Department of Geosciences, University of Copenhagen). The wavelength of X-ray used for measurement was 1.54059 Å. The separated portions of samples for PXRD were usually in very small quantities (≤20 mm^3). They were therefore mounted as thin layers on specially cut single-crystal quartz plates that produce no scattering inside the instrument's measuring range that was 5° to 70° or 90° 2θ, with measurement steps of 0.02° and sufficient measuring time for producing good diffraction patterns (usually 4 s per step). The identification of minerals was done with the help of the JCPDS powder diffraction database (ICDD product) and the own set of calculated patterns from the ICSD database (FIZ Karlsruhe product) plus use of the Rietveld method (Topas 4.1 program, Bruker-AXS product). Modern single-crystal diffractometers enable fast analyses of small grains (only several tens of micrometer in diameter). The full crystal structure characterisation they offer is essential in the definition of new mineral species encountered in fumaroles and builds the basis for many of results reported here.

2.3. SEM-EDS

The use of a SEM equipped with EDS (Si(Li), Ge or silicon drift) gives a possibility to obtain very good images by secondary and backscattered electrons together with a chemical micro-analysis. The ED detector has the advantage of providing a full spectrum in a very short time that can be very helpful for quick, preliminary identification of minerals. The high counting efficiency of the solid-state ED detectors allows a complete analysis of a mineral in very short time (50 s or less) and with very low probe currents of the beam (about 500 pA). The low probe current involves the generation of a small X-ray escape volume and therefore accurate analysis of minerals even in the case of crystals of extremely small size and in the co-presence of other mineral phases, without the risk of evaporating the sample. Moreover, an ED detector that

http://dx.doi.org/10.5772/64129

does not require critical positioning of the sample [2, 3] can give good quantitative chemical data analysing directly the natural faces of the crystals without a need of polished surfaces required for microprobe, but mostly impossible for fumarolic samples, which as a rule consist of loose aggregates of tiny crystals. The last generation of solid-state silicon drift detectors (SSD), normally equipped with a very thin polymeric SuperAtmosphere Thin Window©, gives an output signal with much higher count rates that guarantee also a better sensitivity for light elements even at very low probe currents. Their use in conjunction with the newest software for the correction of the matrix effects [4] is highly recommended for the samples of fumarolic minerals.

Our investigations were carried out with two SEM instruments: the Stereoscan 360 of Cambridge Instruments and the EVO-50XVP of Zeiss-Cambridge. Microanalyses were carried out with Oxford-Link Ge ISIS energy dispersive spectrometer or Oxford X-max (80 mm^2) silicon drift detector, both equipped with a SuperAtmosphere Thin Window©. The operating conditions were as follows: 15 kV accelerating potential, 500 pA probe current, counting time 100 s. The software used was Z AF4/FLS and eXtended Pouchou and Pichoir (XPP) correction scheme, respectively, both Oxford-Link Analytical products.

3. The minerals

More than 200 different minerals have been described from European fumaroles. With the rest of the world, the number might be over 300. Most of them are rare or extremely rare but can be important as indicators of specific conditions in the fumarole where they have been found. **Table 1** gives the chemical and crystallographic parameters of the scientifically confirmed European fumarolic minerals. In the following text, we describe the main features of the mineral groups and individual minerals in fumaroles. The exposition of species follows the mineral classification of Strunz [5] with small modifications. Jakobsson et al. [1] listed in their work a number of supposed new minerals and labelled them each with a two-letter symbol. For those that still do not have mineral names, we used the same notation. The labels for the localities are as follows: A (Askja), CF (Campi Flegrei), El (Eldfell), Et (Etna), F (Fimmvörðuháls), H (Hekla), Kr (Krafla), M (Milos), N (Nisyros), Sa (Santorini), So (Soussaki), Su (Surtsey), Ve (Vesuvius), and Vu (Vulcano).

Minerals	Formula	Sp.gr.	Unit cell parameters (Å, °)	ICSD
Sulphur-α^*	S_8	Fddd	10.465 12.866 24.49	63082
Sulphur-β	S_8	$P2_1/c$	10.926 10.855 10.790 95.9	870
rosickýite	S_8	P2/c	8.455 13.052 9.267 124.9	66517
sulphurite*	S+As,Se	amorph		amorph
Selenium-α	Se_8	$P2_1/n$	9.054 9.083 11.601 90.8	2718

Minerals	Formula	Sp.gr.	Unit cell parameters (Å, °)	ICSD
siderazot	Fe_3N	$P6_322$	4.698 4.379	79983
Gold	Au	Fm-3m	4.079	52700
tellurium	Te	$P3_12$	4.456 5.921	65692
covellite	CuS	$P6_3/mmc$	3.796 16.36	41975
sphalerite	ZnS	F-43m	5.409	77082
wurtzite	ZnS	$P6_3mc$	3.823 6.261	67453
chalcopyrite	$CuFeS_2$	I-42d	5.289 10.423	2518
pyrrhotite	$Fe_{11}S_{12}$	Cc	6.897 11.954 17.702 101.3	166063
millerite	NiS	R3m	9.611 3.151	151599
galena*	PbS	Fm-3m	5.934	38293
pyrite*	FeS_2	Pa-3	5.416	109377
realgar*	As_4S_4	$P2_1/n$	9.325 13.571 6.587 106.4	15238
pararealgar	As_4S_4	$P2_1/c$	9.909 9.655 8.502 97.29	80125
alacranite1	As_8S_9	P2/c	9.942 9.601 9.178 101.9	98792
alacranite2	As_4S_4	C2/c	9.943 9.366 8.908 102.0	95290
dimorphite-α (HT)	As_4S_3	Pnma	9.158 8.033 10.200	188058
dimorphite-β (LT)	As_4S_3	Pnma	11.217 9.922 6.607	188059
demicheleite	BiS(Br,Cl,I)	Pnam	8.042 9.851 4.033	161637
bismuthinite*	Bi_2S_3	Pnma	11.269 3.972 11.129	153946
mozgovaite	$PbBi_4(S,Se)_7$	Bbmm?	13.18 37.4 4.05?	[28]
galenobismutite*	$PbBi_2S_4$	Pnam	11.802 14.569 4.076	158392
cannizzarite*	$Pb_{48}Bi_{56}(S_{1-x}Se_x)_{132}$	$P2_1/m$	38.87 4.090 39.84 102.3	169960
cosalite	$Pb_2Bi_2S_5$	Pnma	23.89 4.062 19.143	169944
lillianite	$Pb_3Bi_2S_6$	Bbmm	13.540 20.64 4.110	246062
heyrovskyite	$Pb_6Bi_2S_9$	Bbmm	13.719 31.39 4.132	180078
kirkiite	$Pb_{10}Bi_3As_3S_{19}$	$P2_1/m$	8.700 26.24 8.774 119.7	156249
vurroite	$Pb_8(Pb,Bi)_2(Sn,Bi)(As,Bi,Pb)(Bi,As)_{10}S_{27}Cl_3$	C2/c	8.371 45.50 27.27 98.8	160401
sylvite*	KCl	Fm-3m	6.285	165593
halite*	NaCl	Fm-3m	5.620	18189
salammoniac*	NH_4Cl	Pm-3m	3.877	22141
lafossaite	TlCl	Pm-3m	3.901	5253
sellaite	MgF_2	$P4_2/mnm$	4.621 3.052	394
chloromagnesite	$MgCl_2$	R-3m	3.636 17.666	86439

Minerals	Formula	Sp.gr.	Unit cell parameters (Å, °)	ICSD
scacchite	$MnCl_2$	R-3m	3.711 17.59	33752
fluorite*	CaF_2	Fm-3m	5.463	41413
oskarssonite*	$Al(F,OH)_3$	R-3c	4.982 12.387	5243
parascandolaite	$KMgF_3$	Pm-3m	4.003	192409
molysite*	$FeCl_3$	R-3	6.056 17.407	39764
carnallite	$KMgCl_3(H_2O)_6$	Pnna	16.119 22.47 9.551	64691
eriochalcite	$CuCl_2(H_2O)_2$	Pbmn	7.414 8.089 3.746	40290
ammineite	$CuCl_2(NH_3)_2$	Cmcm	7.688 10.645 5.736	180189
chloraluminite	$AlCl_3(H_2O)_6$	R-3c	11.827 11.895	22071
ferruccite	$NaBF_4$	Cmcm	6.837 6.262 6.792	36067
avogadrite	KBF_4	Pnma	8.659 5.480 7.030	9875
barberiite	NH_4BF_4	Pnma	9.077 5.679 7.279	9918
rosenbergite	$AlF_3(H_2O)_3$	P4/n	7.715 3.648	66691
HI	$FeF_3(H_2O)_3$	P4/n	7.846 3.877	14134
HU	$FeF_3(H_2O)_3$	R-3	9.253 4.675	unp
pachnolite	$NaCaAlF_6H_2O$	Fd	12.117 10.414 15.680 90.4	40132
gearksutite	$CaAlF_4(OH)H_2O$	P-1	4.94 6.81 6.978 101.1 94.9 110.1	89800
jakobssonite*	$CaAlF_5$	C2/c	8.601 6.290 7.219 114.6	188924
leonardsenite*	$MgAlF_5(H_2O)_2$	Imma	7.064 10.131 6.774	411650
HG	$Na_2Ca_3Al_2F_{14}$	$I2_13$	10.257	202657
coulsellite	$CaNa_3AlMg_3F_{14}$	R-3m	7.161 17.594	168054
thermessaite	$K_2AlF_3SO_4$	Pbcn	10.810 8.336 6.822	161272
thermessaite-(NH_4)	$(NH_4)_2AlF_3SO_4$	Pbcn	11.301 8.612 6.850	[45]
ralstonite*	$Na_xMg_xAl_{2-x}(F,OH)_6(H_2O)_y$	Fd-3m	9.91	31345
HH	$Ca_3Al_2F_{10}(OH)_2(H_2O)_3$?	C2/m?	6.257 22.19 6.311 115.5 (?)	unp
HB	Na-Ca-Al-F?	?	?	[1]
HD*	$(NH_4)_xFe_2F_6$	Fd-3m	10.325	202047
meniaylovite	$Ca_4AlSi(SO_4)F_{13}(H_2O)_{12}$	Fd-3	16.71	100728
cossaite	$Mg_{0.5}Al_6H(SO_4)_7F_6(H_2O)_{33}$	R-3	22.01 9.238	188928
malladrite*	Na_2SiF_6	P1	8.859 8.859 5.038 90 90 120	40917
hieratite	K_2SiF_6	Fm-3m	8.134	29407
demartinite	K_2SiF_6	$P6_3mc$	5.646 9.232	158483
heklaite*	$KNaSiF_6$	Pnma	9.339 5.503 9.796	183232

Minerals	Formula	Sp.gr.	Unit cell parameters (Å, °)	ICSD
cryptohalite*	$(NH_4)_2SiF_6$	Fm-3m	8.395	18033
bararite	$(NH_4)_2SiF_6$	P-3m	5.784 4.796	18027
HT	$FeSiF_6(H_2O)_6$	R-3m	9.616 9.675	41535
knasibfite	$K_3Na_4(SiF_6)_3BF_4$	Imm2	5.522 17.106 9.175	160430
chlormanganokalite	K_4MnCl_6	R-3c	11.926 14.787	24475
erythrosiderite	$K_2FeCl_5H_2O$	Pnma	13.75 9.92 6.93	30321
kremersite	$(NH_4)_2FeCl_5H_2O$	Pnma	13.706 9.924 7.024	200322
mitscherlichite	$K_2CuCl_4(H_2O)_2$	$P4_2/mnm$	7.477 7.935	16052
melanothallite	Cu_2OCl_2	Fddd	7.469 9.597 9.700	96610
atacamite*	$Cu_2Cl(OH)_3$	Pnma	6.030 6.865 9.120	61252
paratacamite*	$Cu_2Cl(OH)_3$	R-3	13.654 14.041	1810
connellite	$Cu_{36}Cl_{7.86}(SO_4)_{0.67}(NO_3)_{0.5}(OH)_{62.3}(H_2O)_{5.6}$	$P6_3/mmc$	15.787 9.101	415129
cumengeite	$Pb_{21}Cu_{20}Cl_{42}(OH)_{40}(H_2O)_6$	I4/mmm	15.101 24.49	157067
bismoclite	BiOCl	P4/nmm	3.887 7.354	74502
lucabindiite	$(K,NH_4)As_4O_6((Cl,Br)$	P6/mmm	5.239 9.014	289996
cotunnite	$PbCl_2$	Pnam	7.619 9.043 4.534	202130
pseudocotunnite	K_2PbCl_4	?	?	[10]
challacolloite*	KPb_2Cl_5	$P2_1/c$	8.849 7.918 12.472 90.1	416430
hephaistosite	$TlPb_2Cl_5$	$P2_1/c$	9.003 7.972 12.569 90.05	166293
brontesite	$(NH_4)_3PbCl_5$	Pnma	8.435 15.773 8.445	166092
panichiite	$[NH_4)_2SnCl_6$	Fm-3m	10.064	163660
steropesite	Tl_3BiCl_6	Cc	26.69 15.127 13.014 108.1	163661
argesite	$[NH_4)_7Bi_3Cl_{16}$	R-3c	13.093 102.68	5283
tenorite	CuO	C2/c	4.684 3.423 5.129 99.5	16025
spinel	$MgAl_2O_4$	Fd-3m	8.089	40030
magnesioferrite	$MgFe_2O_4$	Fd-3m	8.394	158402
magnetite	Fe_3O_4	Fd-3m	8.396	30860
hausmannite	Mn_3O_4	$I4_1/amd$	5.765 9.442	68174
minium	Pb_3O_4	$P4_2/mbc$	8.811 6.563	4106
corundum	Al_2O_3	R-3c	4.761 12.995	9770
hematite*	Fe_2O_3	R-3c	5.035 13.749	82904
ilmenite	$FeTiO_3$	R-3	5.088 14.085	30664
pseudobrookite	Fe_2TiO_5	Ccmm	9.793 3.730 9.976	51225

Minerals	Formula	Sp.gr.	Unit cell parameters (Å, °)	ICSD
opal*	$SiO_2(H_2O)_x$	amorph		amorph
cristobalite*	SiO_2	$P4_12_12$	4.978 6.948	9327
tridymite	SiO_2	Cc	18.494 4.991 23.76 105.8	1109
quartz*	SiO_2	$P3_22$	4.913 5.405	174
anatase	TiO_2	$I4_1/amd$	3.784 9.515	9852
rutile	TiO_2	$P4_2/mnm$	4.592 2.957	33837
akaganeite	$FeOOHCl_x$	I2/m	10.600 3.034 10.513 90.2	69606
portlandite	$Ca(OH)_2$	P-3m	3.585 4.895	15471
gibbsite	$Al(OH)_3$	$P2_1/n$	8.684 5.078 9.736 94.5	6162
doyleite	$Al(OH)_3$	P-1	5.00 5.168 4.983 97.4 118.7 104.7	50581
calcite*	$CaCO_3$	R-3c	4.988 17.061	40107
magnesite	$MgCO_3$	R-3c	4.635 15.019	40117
dolomite*	$CaMg(CO_3)_2$	R-3	4.806 16.006	66333
hydromagnesite	$Mg_5(CO_3)_4(OH)_2(H_2O)_4$	$P2_1/c$	10.105 8.954 8.378 114.4	920
aragonite	$CaCO_3$	Pmcn	4.961 7.970 5.742	166085
cerussite	$PbCO_3$	Pmcn	5.180 8.492 6.134	6178
azurite	$Cu_3(CO_3)_2(OH)_2$	$P2_1/c$	5.011 5.850 10.353 92.4	158577
thermonatrite	$Na_2CO_3H_2O$	$P2_1ab$	6.472 10.724 5.259	1852
natron	$Na_2CO_3(H_2O)_{10+x}$	Cc	12.750 9.001 12.590 115.8	97924
trona	$Na_3H(CO_3)_2(H_2O)_2$	C2/c	20.41 3.493 10.333 106.5	192710
sassolite*	H_3BO_3	P-1	7.039 7.053 6.578 92.6 101.2 119.8	24711
metaborite	HBO_2 (HT>140°C)	P-43n	8.886	34639
clinometaborite	HBO_2 (LT)	$P2_1/a$	7.127 8.842 6.773 93.2	183581
ameghinite	$NaB_3O_3(OH)_4$	C2/c	18.428 9.882 6.326 104.4	4219
chalcocyanite	$CuSO_4$	Pnma	8.409 6.709 4.833	71017
vanthoffite	$Na_6Mg(SO_4)_4$	$P2_1/c$	9.797 9.217 8.199 113.5	16607
EN	$Na_3Al(SO_4)_3$	R-3	13.376 8.933	unp
EA	$NaMgAl(SO_4)_3$	R-3	8.303 21.87	unp
EI	$Na_2Mg_2(SO_4)_3$	?	?	unp
langbeinite*	$K_2Mg_2(SO_4)_3$	$P2_13$	9.921	40986
manganolangbeinite	$K_2Mn_2(SO_4)_3$	$P2_13$	10.114	200897
steklite	$KAl(SO_4)_2$	P321	4.728 8.001	[75]
pyracmonite	$(NH_4)_3Fe(SO_4)_3$	R3c	15.217 8.932	169964

Minerals	Formula	Sp.gr.	Unit cell parameters (Å, °)	ICSD
aluminopyracmonite	$(NH_4)_3Al(SO_4)_3$	R-3	15.032 8.878	190666
eldfellite	$NaFe(SO_4)_2$	C2/m	8.043 5.139 7.115 92.1	166768
yavapaiite	$KFe(SO_4)_2$	C2/m	8.150 5.162 7.855 94.9	26004
thenardite*	Na_2SO_4	Fddd	5.860 12.304 9.817	2895
metathenardite*	Na_2SO_4 (HT)	$P6_3/mmc$	5.326 7.126	63077
aphthitalite*	$KNaSO_4$	P3m	5.607 7.177	26014
glaserite	$K_3Na(SO_4)_2$	P-3m	5.680 7.309	26018
palmierite	$K_2Pb(SO_4)_2$	R-3m	5.497 20.86	94234
mascagnite	$(NH_4)_2SO_4$	Pnam	7.782 10.636 5.993	34257
mercallite	$KHSO_4$	Pbca	8.415 9.796 18.967	249738
FB	$Na_3H(SO_4)_2$	$P2_1/c$	8.644 9.641 9.139 108.8	249553
therasiaite	$(NH_4)_3KNa_2Fe_2(SO_4)_3Cl_5$	Cc	18.284 12.073 9.535 108.1	5296
anhydrite*	$CaSO_4$	Amma	6.991 6.996 6.238	15876
gypsum*	$CaSO_4(H_2O)_2$	C2/c	6.277 15.181 5.672 114.1	161622
bassanite	$CaSO_4(H_2O)_{0.5}$	C2	17.559 6.962 12.070 133.4	380286
omongwaite	$Na_2Ca_5(SO_4)_6(H_2O)_3$	C2	12.089 6.903 6.354 90.1	88942
glauberite	$CaNa_2(SO_4)_2$	C2/c	10.129 8.306 8.533 112.2	16901
barite	$BaSO_4$	Pbnm	7.154 8.879 5.454	76926
celestite	$SrSO_4$	Pbnm	6.867 8.354 5.346	92608
anglesite	$PbSO_4$	Pbnm	6.955 8.472 5.397	92609
dolerophanite	Cu_2OSO_4	C2/m	9.370 6.319 7.639 122.3	61513
antlerite	$Cu_3SO_4(OH)_4$	Pnma	8.289 6.079 12.057	96348
d'ansite	$Na_{21}Mg(SO_4)_{10}Cl_3$	I-43d	15.90	[86]
d'ansite-(Mn)	$Na_{21}Mn(SO_4)_{10}Cl_3$	I-43d	15.929	190535
d'ansite-(Fe)	$Na_{21}Fe(SO_4)_{10}Cl_3$	I-43d	15.882	190536
aiolosite	$Na_4Bi(SO_4)_3Cl$	$P6_3/m$	9.626 6.880	166960
natroalunite*	$(Na,K)Al_3(SO_4)_2(OH)_6$	R-3m	6.973 16.877	166305
alunite*	$KAl_3(SO_4)_2(OH)_6$	R-3m	7.020 17.223	12106
natrojarosite	$NaFe_3(SO_4)_2(OH)_6$	R-3m	/.315 16.587	160409
jarosite*	$KFe_3(SO_4)_2(OH)_6$	R-3m	7.315 17.224	12107
adranosite	$(NH_4)_4NaAl_2(SO_4)_4Cl(OH)_2$	$I4_1/acd$	18.118 11.320	169963
adranosite-(Fe)	$(NH_4)_4NaFe_2(SO_4)_4Cl(OH)_2$	$I4_1/acd$	18.261 11.562	[90]
euchlorine*	$KNaCu_3O(SO_4)_3$	C2/c	18.41 9.43 14.21 113.7	69451

Minerals	Formula	Sp.gr.	Unit cell parameters (Å, °)	ICSD
chlorothionite	$K_2CuSO_4Cl_2$	Pnma	7.732 6.078 16.292	22364
linarite	$PbCuSO_4(OH)_2$	$P2_1/m$	9.701 5.650 4.690 102.6	68173
baliczunicite	$Bi_2O(SO_4)_2$	P-1	6.739 11.184 14.175 80.1 88.5 89.5	[13]
leguernite	$Bi_{38}O_{42}(SO_4)_{15}$	P2	11.249 5.657 11.914 99.2	[91]
kieserite	$MgSO_4H_2O$	C2/c	6.891 7.624 7.645 117.7	68345
rozenite*	$FeSO_4(H_2O)_4$	$P2_1/n$	5.979 13.648 7.977 90.4	23912
chalcanthite	$CuSO_4(H_2O)_5$	P-1	6.116 10.716 5.961 82.4 107.3 102.6	20657
pentahydrite	$MgSO_4(H_2O)_5$	P-1	6.314 10.565 6.030 81.1 109.8 105.1	2776
hexahydrite*	$MgSO_4(H_2O)_6$	C2/c	10.110 7.212 24.41 98.3	16546
nickelhexahydrite	$NiSO_4(H_2O)_6$	C2/c	9.880 7.228 24.13 98.4	65018
römerite*	$Fe_3(SO_4)_4(H_2O)_{14}$	P-1	6.463 15.309 6.341 90.5 101.1 85.7	15207
coquimbite	$(Fe,Al)_2(SO_4)_3(H_2O)_9$	P-31c	10.937 17.081	169956
halotrichite*	$FeAl_2(SO_4)_4(H_2O)_{22}$	$P2_1/c$	6.195 24.26 21.26 100.3	96598
pickeringite	$MgAl_2(SO_4)_4(H_2O)_{22}$	$P2_1/c$	6.184 24.27 21.23 100.3	90028
meta-alunogen	$Al_2(SO_4)_3(H_2O)_{14}$	?	?	[43]
alunogen*	$Al_2(SO_4)_3(H_2O)_{17}$	P-1	7.42 26.97 6.062 89.6 97.3 91.5	12129
mirabilite	$Na_2SO_4(H_2O)_{10}$	$P2_1/c$	11.474 10.356 12.788 107.8	411348
campostriniite	$(NH_4,K)_2Bi_{2.5}Na_{2.5}(SO_4)_6{\cdot}H_2O$	C2/c	17.748 6.982 18.221 114.0	[92]
rhomboclase*	$FeH(SO_4)_2(H_2O)_4$	Pnma	9.742 18.333 5.421	183662
voltaite*	$K_2Fe_8Al(SO_4)_{12}(H_2O)_{18}$	Fd-3c	27.25	9254
löweite	$Na_{12}Mg_7(SO_4)_{13}(H_2O)_{15}$	R-3	18.924 13.538	15209
eugsterite	$Na_4Ca(SO_4)_3(H_2O)_2$	?	?	[93]
hydroglauberite	$Ca_3Na_{10}(SO_4)_8(H_2O)_6$	?	?	[94]
syngenite	$K_2Ca(SO_4)_2H_2O$	$P2_1/m$	9.771 7.145 6.247 104.0	157072
kröhnkite	$Na_2Cu(SO_4)_2(H_2O)_2$	$P2_1/c$	5.518 12.666 5.808 108.4	422593
ferrinatrite	$Na_3Fe(SO_4)_3(H_2O)_3$	P-3	15.560 8.666	14003
cyanochroite	$K_2Cu(SO_4)_2(H_2O)_6$	$P2_1/a$	9.066 12.13 6.149 104.4	2925
bloedite	$Na_2Mg(SO_4)_2(H_2O)_4$	$P2_1/a$	11.135 8.248 5.542 100.8	151453
polyhalite	$K_2Ca_2Mg(SO_4)_4(H_2O)_2$	F-1	11.690 16.330 7.600 91.6 90 91.9	6304
tamarugite*	$NaAl(SO_4)_2(H_2O)_6$	$P2_1/a$	7.353 25.22 6.097 95.2	15187
picromerite	$MgK_2(SO_4)_2(H_2O)_6$	$P2_1/a$	9.072 12.212 6.113 104.8	26772

Minerals	Formula	Sp.gr.	Unit cell parameters (Å, °)	ICSD
metavoltine	$K_2Na_6Fe^{2+}Fe_6^{3+}O_2(SO_4)_{12}(H_2O)_{18}$	P3	9.575 18.17	8270
kalinite	$KAl(SO_4)_2(H_2O)_{11}$	C2/c	19.92 9.27 8.304 98.8	[95]
alum-(K)	$KAl(SO_4)_2(H_2O)_{12}$	Pa-3	12.164	280548
kainite	$KMgSO_4Cl(H_2O)_{2.75}$	C2/m	19.72 16.23 9.53 94.9	26003
SH	$Na_2Mg_3(SO_4)_2(OH)_2(H_2O)_4$	$Cmc2_1$	19.735 7.223 10.028	425875
chessexite	$Na_4Ca_2Mg_3Al_8(SiO_4)_2(SO_4)_{10}(OH)_{10}(H_2O)_{40}$	?	?	[96]
chlorapatite	$Ca_5(PO_4)_3(Cl,OH)$	$P6_3/m$	9.564 6.816	1706
mimetite	$Pb_5(AsO_4)_3Cl$	$P6_3/m$	10.240 7.440	188080
phoenicochroite	Pb_2OCrO_4	C2/m	14.001 5.675 7.137 115.2	34831

Chemical formula, space group, unique unit cell parameters and the ICSD identification number (ICSD = Inorganic Crystal Structure Database, Fachinformationszentrum Karlsruhe, Germany). For the species that still lack ICSD entry, the reference is given as a citation, as unp = unpublished data, or amorph = amorphous compound. Minerals common in fumaroles are marked with a star.

Table 1. Minerals from European fumaroles.

3.1. Elements

Sulphur is the most abundant native element in fumaroles and generally one of the most common minerals in this environment. It appears in the following various forms: as thick yellow blocky crystalline masses, well-formed crystals (in cavities or on surfaces), granular crusts and acicular spear-like dendritic crystals (at vents of fumaroles, **Figure 2**) or as an admixture to earthy altered rock material, giving it grey colour. Sulphur forms through oxidation of H_2S. It is typically accompanied by alunite, gypsum or salammoniac, but it is also found in other associations. The molecules in the crystal structure consist of puckered eight-member rings of atoms in all three polymorphs found in nature. Native sulphur or α-sulphur is orthorhombic and at atmospheric pressures stable up to 95°C when it transforms reversibly to the monoclinic β-form with the melting temperature of 119°C. It can therefore be supposed that a significant part of sulphur found in fumaroles was formed as the high-temperature form and on cooling transformed to the alpha form observed typically on XRD diagrams. As solid unstable over 120°C, sulphur can be found only in the low-temperature fumaroles or at the outer rims of the hotter ones. It was found on all localities except F.

Rare: **Rosickýite or γ-sulphur**: observed once in a small transparent green-yellow crust made of platy crystals (Vu [6]). Metastable at all temperatures [7]. Conditions of formation still not completely understood. **Sulphurite**, amorphous S with As and Se, Vu [8]. **Selenium**: observed as red crusts (Ve [9], Vu [10]) and so it seems that it was the metastable form, which contains ring molecules similar to that of sulphur and not the stable polymorph with infinite spiral molecules, which is metallic in appearance. Melts at 217°C. **Siderazote**, Ve [9]: iridiscent cover

on lavas. **Gold** and **tellurium**, Vu [11], observed as several micrometer-sized grains in the silicic alteration zone of the crater.

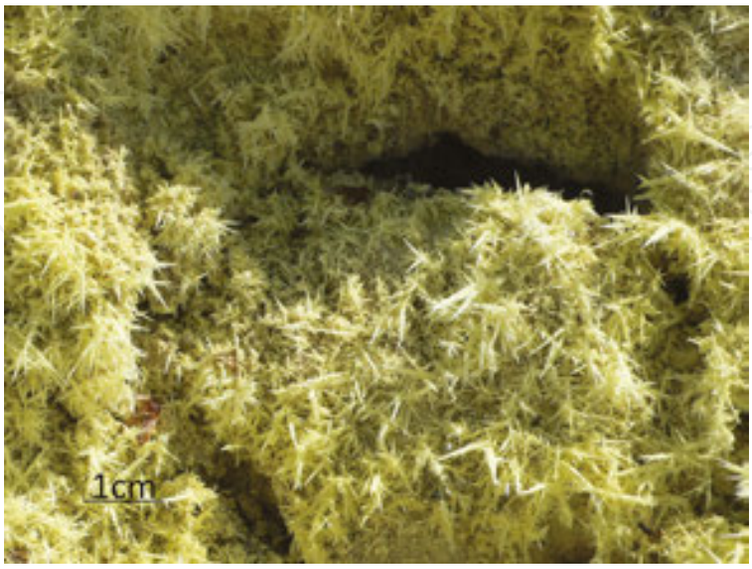

Figure 2. Spear-like crystals of sulphur. Fumarole on Nisyros.

3.2. Sulphides

Metallic sulphides are confined to deeper parts of a volcanic system with its high-temperature hydrothermal conditions and rarely appear as sublimates and then in small amounts on the surface of the fumaroles. Here, their formation depends on the persistence of reducing conditions in parts of these largely fluctuating systems. These were especially characteristic for Vesuvius in the periods immediately following the eruptions and for Vulcano during the thermal "crisis" (temperature increase in the fumaroles). Semimetals form stronger covalent bonds with sulphur and are more volatile, and therefore, they can appear in fumaroles in significant quantities either as simple sulphides or, when combining with metals, as sulphosalts (see below). Observed in the investigated localities are As and Bi, whereas Sb did not appear in quantities sufficient to form its minerals. Arsenic forms discrete molecules with sulphur and its simple sulphides are confined to low-temperature hydrothermal deposits and low-temperature fumaroles where they can appear in important quantities (CF). On Vulcano, however, it is mostly a constituent of sulphosalts together with Bi. The transport of the latter is supposed to occur as Bi-Cl complexes, so the abundance of its sulphides, sulphosalts and other minerals in the fumaroles of Vulcano is interpreted as a combined action of both elements [12].

Rare: **Covellite**, Ve [9]: deep-blue thin crusts. **Sphalerite**, Vu [13]: Cd-rich, in HT association of sulphides and sulphosalts. **Wurtzite**, Vu [13]: Metastable under 1020°C, accompanies sphalerite. **Chalcopyrite**, Ve [9]: metallic thin crusts composed of minute crystals. **Pyrrhotite**, Ve [14], Vu [13]: metallic hexagonal lamellae. **Millerite**, Ve [9]: observed once in capillary

crystals. **Galena**, Ve [9]: with Fe-sulphides and oxides; Vu [12]: Se-rich, in company of Bi-Pb sulphosalts of the similar silver colour and metallic lustre. **Pyrite**, Vu [13], Ve [9]: with other sulphides; CF [15]: minute crystals dispersed in altered tuffs; So: in opalized rock; M: in microcrystals with rhomboclase and voltaite.

As-sulphides realgar, pararealgar, alacranite and **dimorphite** have molecular crystal structures with As_4S_n cage molecules. The commonest of them is **realgar (Figure 3)**. As_4S_4 melts at 309°C [16] and is therefore confined to low-to-intermediate *T* fumaroles. CF [17]: the main constituent in a fumarole on Solfatara in grainy or crusty aggregates of sub-mm prismatic light red lustrous crystals associated with salammoniac; Ve [9]: rare small red crystals associated with sulphur and selenium. Realgar transforms under the influence of visible or UV light into the orange-yellow **pararealgar** [18], earlier often mistaken for orpiment. CF: it is the alteration product of realgar. The synthetic HT polymorph β-As_4S_4 is stable over 267°C [16]. In natural occurrences, this type of molecule is partly substituted by As_4S_5 until the 1:1 proportion as in the type specimen of **alacranite (As_8S_9)** that has the ordered arrangement of the two types of molecules and different symmetry than β-As_4S_4 [19]; CF [20]: orange small crystals with realgar and dimorphite. **Dimorphite** has two polymorphs. LT β-form transforms to HT α-form at 130°C [21], which melts at 211°C [16]. CF, Ve [17]: tiny orange or yellow crystals with adamantine lustre. **Demicheleite** (Vu [22–24]) is a solid solution with three end-members containing different halogene elements (Cl, Br, I). Very rare prismatic red to black sub-mm crystals associated with other Bi minerals.

Figure 3. Realgar, Solfatara. Sample from the Natural History Museum in Copenhagen.

3.3. Sulphosalts

Sulphosalts, sulphides containing thioarsenide, thioantimonide, or thiobismuthite group(s), are relatively rare constituents of fumaroles. Among the fumaroles reported here, they appear

http://dx.doi.org/10.5772/64129

only on Vulcano where they were abundant during the "thermal crises" when the fumarolic temperatures exceeded approximately 450°C. Recent analysis of the roots of paleofumarole at El Indio, Chile, revealed subsurface formation of sulphosalts crystallized from a melt condensing from hot fumarolic gases [25]. We could expect the same situation in the roots of the fumaroles on Vulcano during the periods of lower gas dynamics. When it increased during the thermal crisis, the hot front of the sulphosalt formation reached the surface and this established the new thermodynamical conditions where their crystals formed as sublimates at fumarole vents through a quenching process, producing generally very small crystals, homogeneous and lacking traces of decomposition [26]. They are silver-grey in colour, with metallic lustre and acicular (the latter with the exceptions of kirkiite and cannizzarite). A simple sulphide bismuthinite is here described together with sulphosalts because of its close structural and genetic relation to these minerals.

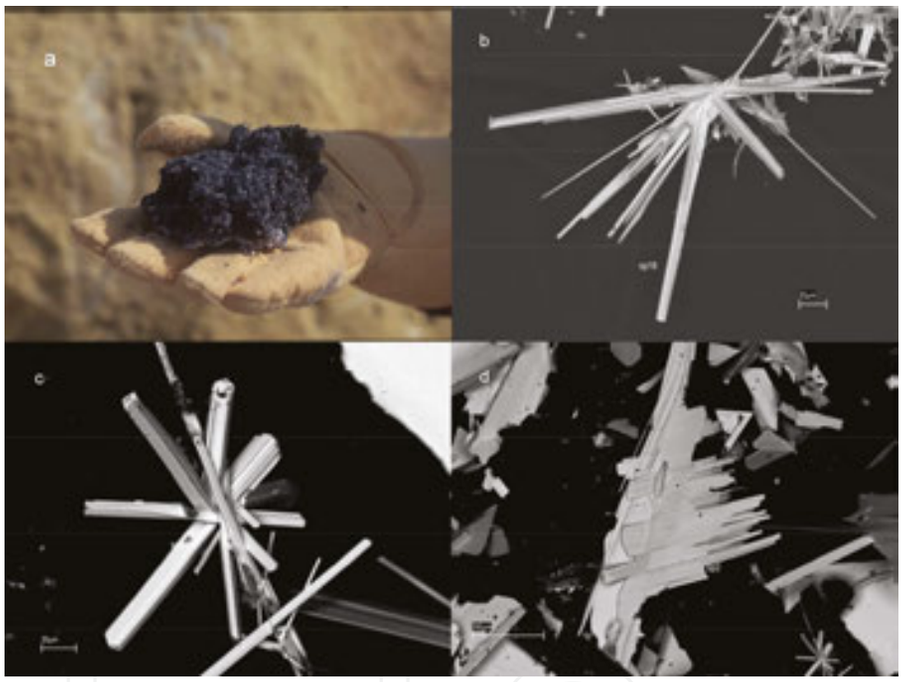

Figure 4. (a) A sample with sulphosalts, Vulcano; (b) SEM photograph of vurroite; (c) SEM photograph of bismuthinite and (d) SEM photograph of cannizzarite.

Sulphosalts belonging to the PbS-Bi_2S_3 system predominate on Vulcano due to high concentration of Pb and Bi in the gases, transported as volatile chlorides or chlorosulphide complexes [12]. **Bismuthinite** is relatively common and with galena mixed with Pb-Bi sulphosalts [27]. **Mozgovaite** [28] is known only from Vulcano and very rare. **Galenobismutite** is fairly common [12]. **Cannizzarite** [27] is a mineral with an incommensurate structure, which gives it a complex stoichiometry, large unit cell and specific crystal form (thin long leaves reaching sometimes mm diameters but only tens of microns thick). It is relatively abundant. **Cosalite** is rare [12] like **lillianite** [29]. The crystal structure of the latter typifies a homologous series [30] where also the rare **heyrovskyite** [31] with a higher Pb/Bi proportion belongs. Some new or very rare minerals were formed by the admixture of other elements to the Bi-Pb sulphosalts.

Kirkiite [32] and **vurroite** [33] are characterized by a partial substitution of Bi by As in the crystal structure, a feature rare in hydrothermal sulphosalt minerals. The former appears in short prismatic crystals and the latter in slender needle-like crystals, both among the smallest crystals in this sulphosalt association. The sulphosalts from Vulcano are specific in having small amounts of Se substituting for S. Another unusual feature is that some of them have also Cl substituting for S (galenobismutite, lillianite) [26] or playing a distinct role in the crystal structure (vurroite) [34] (**Figure 4**).

3.4. Halides

Halides are abundant in some fumaroles and some of them appear commonly in fumaroles (e.g. halite and salammoniac). Where the halides are abundant, they usually appear with a number of species many of which are unique for the fumarolic environment or have it as the main mode of occurrence. As compounds with predominately ionic bonding, they mostly are colourless or light colour and are relatively soft. Characteristic for fluorides in fumaroles is the partial substitution of F by OH. In chlorides, the substitution of OH for Cl is rare or non-existing due to the difference in ionic sizes. When present together, Cl, OH, and O play distinct structural roles and form oxy- or hydroxychlorides. Br and I often partly substitute Cl. Among complex fluorides, the groups of borofluorides, aluminofluorides, and silicofluorides can be defined. Finally, halides in combination with other anions, usually of complex type (like $[SO_4]^{2-}$) also exist in fumaroles. Degassing dynamics of Cl, F and other halogens is a complex function of physical and chemical magma conditions [35] and can vary largely between different volcanoes. Cl generally degasses faster than F [36] and the abundance of H_2O enhances it further [37], which can produce a temporal segregation of the major amounts of chlorides and fluorides in the fumaroles after volcanic eruptions. This, however, can be modified if other sources than magma contribute to gas production. Significant amounts of fluorides appear in most of the Icelandic volcanoes. They are less abundant, but still in important quantities on Vulcano, whereas they are rarer on Vesuvius and Etna. Alumino-fluorides are characteristic for all Icelandic volcanoes (except Askja that does not have registered fluorides). Fumaroles on Hekla contain also significant silicofluorides. They are found on Vulcano as well, but here more characteristic are borofluorides. Contrary to fluorides, chlorides are more important in Italian fumaroles (especially Vesuvius and Vulcano) than in Icelandic ones. On Icelandic volcanoes, they were present in important quantities in the first fumaroles after the eruptions, but a decrease with time is also observed while fumaroles still were producing significant amounts of fluorides (El, H). An important thermodynamic distinction exists between the most abundant chlorides in fumaroles, where those of alkali elements represent the high-temperature product, whereas salammoniac characterizes the low-temperature fumaroles. The border line is approximately at 300°C.

Sylvite and **halite** form a complete solid solution at temperatures higher than approximately 480°C and limited solid solution at lower temperatures with higher solubility of Na in sylvine than K in halite. This is often observed in fumaroles and can be deduced from the shift of the powder diffraction maxima. Halite is much more abundant than sylvite. Su [1]: in crusts and stalactites with Ca and Na sulphates. F: crusts or powdery covers of sub-mm cubic crystals

with anhydrite, gypsum and other sulphates. Ve [9]: halite and sylvite are present in high-temperature "dry fumaroles" as earthy or dendritic crusts, rarely as crystals. Et [38]: Halite appears in stalactites and concretions in volcanic tubes accompanied by sylvite; El, H, A, Kr: halite is common in crusts on lava [39].

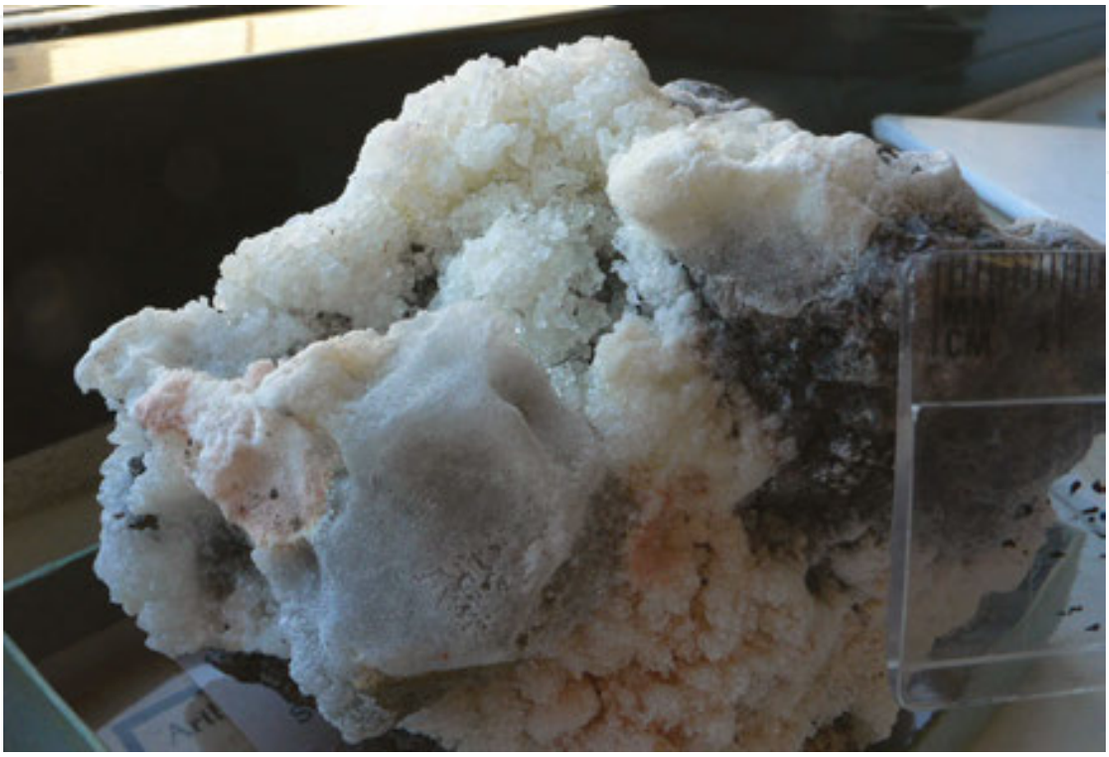

Figure 5. Salammoniac, Etna. Sample from the Natural History Museum in Copenhagen.

Salammoniac (CsCl structure type) (**Figure 5**) is one of the characteristic minerals in low-temperature fumaroles. Its sublimation temperature is 338°C. El [1]: the main constituent of white and yellowish crusts on lava shortly after eruption, but 15 years later no more present. H [1]: one of the main first fumarolic minerals, but already after one year disappeared from the fumaroles. Ve [14]: the representative main mineral of a type of fumaroles mostly on lower lava flows and rarely close to the crater with the temperature around 300°C. Vu [40]: the enrichment in Br follows the enrichment in the magmatic component of the gases. Crusts and aggregates of colourless soft isometric crystals sometimes reaching mm size. Also A, Kr, CF, Et. Typical accompanying minerals are cryptohalite (El, H) sassolite and sulphur (Vu), mascagnite and As sulphides (CF). Isostructural is **lafossaite** [41]; Vu: small grey-brown crystals (<100 μm) covering sulphosalts and pyrite or as opaque crusts; Ve [42]: <100 μm colourless cubic crystals, very rare.

Sellaite, El: in a brown crust with ralstonite and fluorite covering white microcrystalline anhydrite; Ve [43]: in ejected blocks with anhydrite; Et [43]: with fluorite. Very rare. **Chloro-magnesite** and isostructural **scacchite**: very rare, with halite and sylvite (Ve [9]). **Fluorite** is common in fumaroles. Su [1]: the main fluoride in a lava tube and the only fluoride on the

inner wall of a nearly closed crater, but not on the surface of lava where ralstonite is the dominating fluoride. H [1]: it is fairly common but subordinate to ralstonite and jakobssonite. Ve [44]: it is observed on pre-existing tenorite and rare. El: in a brownish crust with ralstonite and sellaite. Very rare. **Oskarssonite** [45] is the stable trigonal low-temperature form of AlF_3 with a perovskite-type framework of AlF_6 octahedra. El: in thick white microcrystalline crusts with other fluorides, opal, and anatase, more abundant than ralstonite in late fumaroles due to decreased amounts of Na and Mg in the gases and rock. Chemical analysis reveals partial replacement of F by OH, consistent with observations by Rosenberg on synthetic material [46]. **Parascandolaite**, Ve [47]: in colourless transparent sub-mm cubic crystals. Very rare.

Molysite Ve [9]: in yellow and red covers of the altered rocks near the crater. **Carnallite**, Su [1]: in a yellow-brown stalactite together with K-enriched halite. **Eriochalcite**, Ve [9]: rare blue wool-like aggregates together with other Cu minerals. **Ammineite**, Ve [48]: bluish crusts on altered tenorite together with opal and artroeite. Very rare. **Chloraluminite**, Ve [14]: small rhombohedral or prismatic crystals in high-temperature fumaroles. Very rare.

Ferruccite and **avogadrite** (Ve [43]) are very rare fumarolic borofluorides. **Barberiite**, Vu [49]: globular aggregates of colourless platy sub-mm crystals. With sulphur, salammoniac, sassolite, malladrite, and realgar.

Rosenbergite, H ([1]: mineral HM): in yellow to brown crusts with other fluorides. Rare. El: secondary hydration phase on oskarssonite. Very rare. **Mineral HI**, isostructural to rosenbergite. H [1]: in yellow to brown crusts together with its polymorph **mineral HU** [1] and other fluorides. Both rare. **Pachnolite**, H [1]: in a yellow/brown/green crust with ralstonite. **Gearksutite**, Vu [50]: in veins, impregnations, pockets, and concretions as alteration product of plagioclase under influence of F-rich solutions; Ve [48]: on post-1944 eruption fumaroles.

Jakobssonite [51] (mineral HA [1]) H, El, F, Kr: white crusts or thin overgrowths of sub-100 μm acicular crystals together with leonardsenite, ralstonite and other alumino- and silicofluorides. Common. Less abundant are **leonardsenite** [52] in orthorhombic-prismatic colourless crystals, and the presumed new mineral **HG** [1] in rhombic-dodecahedral crystals, both sub-100 μm. In similar associations as jakobssonite (H, El). The latter is identical to the synthetic compound of the same composition [53]. **Coulsellite**, Ve [47]: accompanies parascandolaite. **Thermessaite** [54] and **thermessaite-((NH_4))** [55] Vu: in medium temperature fumaroles (around 300°C) in sub-mm colourless prismatic crystals associated with alunite, sassolite, anhydrite, and metavoltine. Very rare.

Ralstonite has a crystal structure consisting of a pyrochlore-type framework of AlF_6 octahedra, with Al partly substituted by Mg, and Na and H_2O in framework cavities [56]. Common, dominating among fluorides in microcrystalline yellow crusts on Iceland (**Figure 6**) (H, El, Su [1]; F, Kr). The presumably new mineral HS [1] (H) shows the same diffraction characteristics as Rosenberg's AHF phase [46] with the composition $Al(F,OH)_3(H_2O)_n$ isostructural to ralstonite. The compositional range of ralstonite is still not sufficiently investigated and it is not clear if HS is a new mineral or a variant of ralstonite. The presumed new mineral **HH** (El, H [1]): thin platy colourless crystals of hexagonal habit up to over 100 μm in diameter in the surface part of the fumaroles. The composition and crystallography are preliminary deter-

mined. Rare. The presumed new mineral **HB** (H, El [1]): in white to yellowish crusts typically with ralstonite. Composition and crystallography unknown. Fairly common. The presumed new mineral **HD** (H, El, Su [1]) is probably an ammonium-free variant [57] of the zeolitic $NH_4Fe^{2+}Fe^{3+}F_6$ with a pyrochlore framework of FeF_6 octahedra [58]. In yellow to brownish crusts mixed with alumino- and silicofluorides. Fairly common. **Meniaylovite**, [59] is a minor constituent in yellow to brownish crusts in association with various other fluorides (Su, El, F, Kr). **Cossaite**, [60] Vu: only two 100 μm crystals found in a medium-T (~350°C) fumarole.

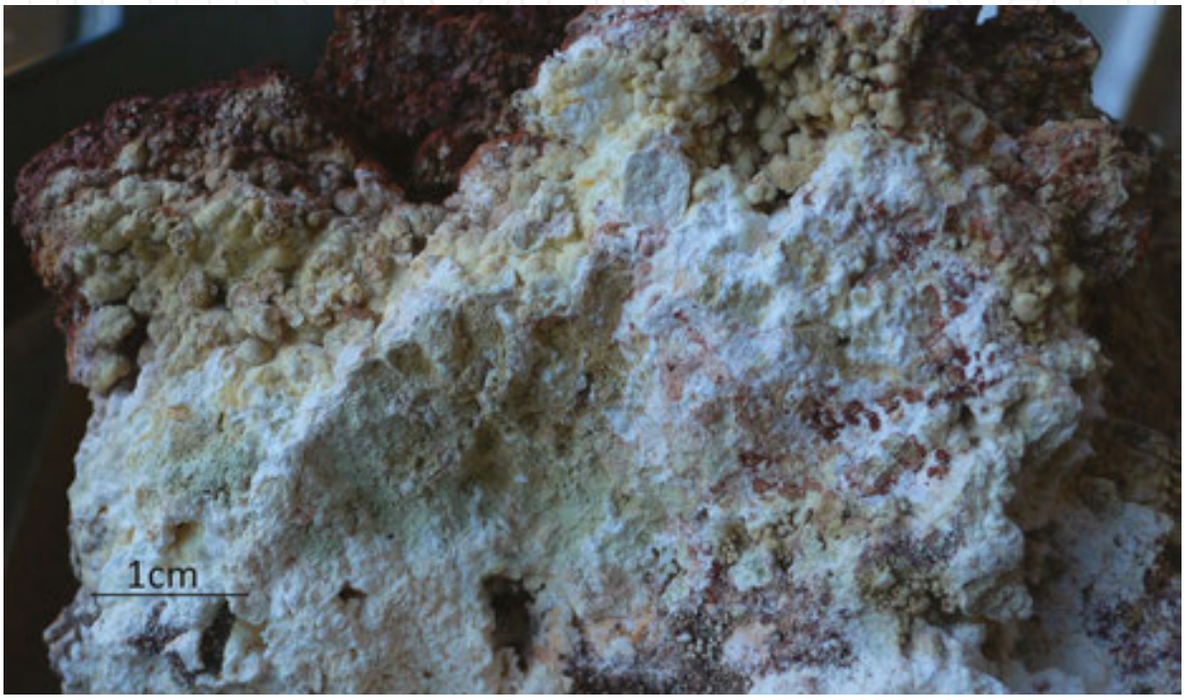

Figure 6. Fluoride crust from Eldfell. Mixture of ralstonite, jakobssonite, oskarssonite and other minor fluorides.

Malladrite, H [1]: fairly common in yellow crusts with ralstonite and jakobssonite; El [1], Kr: rare, in a yellow-brown crust with ralstonite; Vu [49]: rare, in association with barberiite. **Hieratite**, Vu [61]: in small colourless crystals with hexahedral habit associated with sulphur, realgar, sassolite, and several sulphates. Also Ve [43], H [1]. Rare. **Demartinite**, Vu [62] polymorph of hieratite, probably metastable. In colourless hexagonal pyramidal sub-mm crystals. **Heklaite**, H [63]: fairly common with malladrite and sometimes hieratite, because crystal structure differences prevent miscibility of Na and K silicofluorides. **Cryptohalite**, Ve [14]: in colourless cubic or octahedral crystals. Typically follows salammoniac, like on H and El in the first fumaroles [1]. **Bararite** is the low-temperature polymorph of the former, stable under 5°C. Found with salammoniac and cryptohalite (H). Probably a climatic influence. Also Ve [43]. Very rare. Presumed new mineral **HT** [1] is identical with synthetic $FeSiF_6(H_2O)_6$. H: very rare aggregates of micron-sized granular crystals overgrown with aggregates of HU crystals. **Knasibfite**, Vu [64]: with hieratite, avogradite and demartinite in low temperature fumaroles. Very rare.

Chlormanganokalite, Ve [14]: rare yellow crystals in high-temperature fumaroles. **Erythrosiderite**, Ve [14]: rare, in stalactites and crusts of tabular and pseudooctahedral red-orange deliquescent crystals in medium- and high-temperature fumaroles. **Kremersite**, Ve, Vu, Et [43]: rare small orange crusts. **Mitscherlichite**, Ve [43]: very rare in greenish-blue thin crusts. **Melanothallite**, Ve [9]: in rare thin black scales. **Atacamite**, Ve [14]: fairly common in thin green crusts or small prismatic crystals on lava. **Paratacamite**, Ve [9]: fairly common green alteration of tenorite. **Connellite**, Ve [65]: very rare, in post-1994 eruption fumaroles. **Cumengéite**, Ve [44]: very rare small transparent crystals of deep blue colour, adamantine lustre and pseudocuboctahedral habit, with tenorite, gypsum, and cotunnite. **Bismoclite**, Vu [22]: very rare sub-mm brilliant dipyramidal or tabular anatase-like orange crystals. **Lucabindiite**, Vu [8]: rare μm-size platy colourless transparent crystals with samammoniac, sulphur, and arsenolite. **Cotunnite**, Ve [9, 14]: rare colourless lustrous acicular crystals, scales, arborescent aggregates and fused masses, sometimes as pseudomorphs after galena in the high-temperature fumaroles. Vu [66]: variously coloured, fairly common in association with challacolloite. **Pseudocotunnite**, Ve [9]: very rare thin crusts and needles. Not fully crystallographically characterized species. **Challacolloite**, Ve [14]: rare colourless acicular crystals with adamantine lustre in HT fumaroles; Vu [66]: colourless to yellow, red, and brown, fairly common. **Hephaistosite**, Vu [67]: rare aggregates of pale yellow-green tabular crystals associated with Bi and Pb sulphides and chlorides. **Brontesite**, Vu [68]: very rare minute white tabular crystals. **Panichiite**, Vu [69]: very rare minute colourless to pale yellow octahedral crystals with adranosite, alunite, anhydrite. **Steropesite**, Vu [70]: very rare yellow-green minute crystals or crusts covering lafossaite. **Argesite**, [71] Vu: in sub-mm pale yellow very rare crystals in association with bismuthinite.

3.5. Oxides and hydroxides

Oxides are mostly products of reaction of gases with scoria, lava or other rocks in which fumaroles form and in lesser amount form as sublimates. The leaching of lava by aggressive fumarolic gases can lead to material consisting exclusively of oxides of Si, Al, Fe, and Ti, opal-cristobalite, corundum, hematite, and anatase, respectively, mixed with anhydrite (in Icelandic fumaroles) or alunite (in Greek fumaroles).

Tenorite, CuO, Ve [14]: lamellar, leaf-like or fan-like aggregates of crystals of a black metallic appearance in the HT fumaroles (T > 400°C [72]); Et [38]: thin scales with hematite and polyhalite in volcanic tubes. Rare. **Spinel, $MgAl_2O_4$,** El: very rare, in a cellular brown crust consisting mainly of hematite, also accompanied by corundum, anhydrite and steklite. **Magnesioferrite, $MgFe_2O_4$,** and **magnetite, Mg_3O_4,** Ve [9]: minute iron-grey crystals. Rare. **Hausmannite, Mn_3O_4,** Ve [9]: rare thin brown coatings on lavas. **Minium** Ve [9]: very rare dusty red layers cementing volcanic conglomerate. **Corundum**, El: one of the main constituents of the wall rock (with cristobalite, hematite, and anhydrite) of a fumarole (**Figure 7**). **Hematite:** abundant (Su, El, H, F, Ve, Et, M, Sa) and the main reason for the red colour of scoria- and lava-bearing fumaroles. Mostly a decomposition product; also a sublimate in small black crystals with metallic lustre (El). **Ilmenite**, H [1]: in a brownish crust with hematite and

http://dx.doi.org/10.5772/64129

fluorides. **Pseudobrookite**, El: very rare, admixture in a sample of white to grey granular to earthy crust of cristobalite and anhydrite on a substrate of hematite.

Figure 7. Hematite (red) and corundum (white) with opal in the altered lava on Eldfell.

Opal is common in all fumaroles. Primarily a product of decomposition of silicate minerals, but observed amorphous material could also be a primary glassy part of lava. In a sample from El, opal-CT forms the compact part of the leached lava, whereas opal-A fills holes as hydrothermal deposit. Opal is often associated with **cristobalite** (El, CF, Et, So, M, Sa, N) or **tridymite** (Et, Sa, N). They could also be products of fumarolic reactions or just unaltered remnant of lava. **Quartz** is absent in the majority of fumaroles but abundant in some (M, N, El). Mostly remnant of the primary rock, but appearance as granular crust suggests also secondary origin (M). **Anatase:** fairly common in late fumaroles with other oxides (El); rare in the altered rock with quartz, sericite and alunogen (M). Analyses of partly to fully leached lava on Eldfell show that TiO_2 remained as the only other component besides SiO_2 in the opalized rock, which shows it to be relatively immobile [1]. **Rutile**, high-temperature polymorph of TiO_2, stable over 600°C at atmospheric pressures, is rarely observed (M, N) probably primary from lava.

Portlandite, Et [38]: coralloid concretions with calcite in a volcanic tube. **Gibbsite**, Ve [9]: with basanite in hexagonal scales. Its polymorph **doyleite** was confirmed by XRD in one sample from Surtsey, in association with hematite [1].

3.6. Carbonates

Carbonates are rare constituents in fumaroles. It might look strange considering how abundant CO_2 is in volcanic gases, but the scarcity of solid products is due to the typical high acidity of

the fumarolic environments making most carbonates unstable. Where they appear in significant quantities, specific conditions are present, for example, low acidic or even basic environments and high water activity, like in the case of occurrences of Na carbonates on Vesuvius or calcite on Surtsey and Etna.

Calcite is the most frequent carbonate in fumaroles. Common in caves and cavities of lava where steam emanations were vigorous (Su [1]). Fairly common in stalactites and concretions in volcanic tubes (Et [38]). Fairly common in altered rock with **magnesite** and **dolomite** (So [73]). **Hydromagnesite**, Su [1]: in a white botryoidal crust with calcite and fluorite in a lava tube. **Aragonite**, So [73]: rare, with anhydrite and Fe-Mg hydrous sulphates. **Cerussite** accompanies parascandolaite (Ve [47]). **Azurite**, Ve [9]: blue covers on older lavas. **Sodium carbonate hydrates** appear in the high-temperature fumaroles on Vesuvius dominated by potassium and sodium salts [9, 14]; **thermonatrite** in white crusts, sometimes stalactites, **natron** in transparent granules and small translucent crusts as efflorescence in the interior of lavas, and **trona** in small tabular pseudohexagonal crystals or whitish crusts. The latter was also found with halite in concretions in a lava cave on Etna [38].

3.7. Borates

Over 210 boron minerals are known. Among them only three borofluorides mentioned earlier and four borates are observed in fumaroles. The boric acid, **sassolite**, melts at 171°C and is therefore constrained to the low-temperature fumarole. Ve [9]: rare thin colourless scales together with gypsum or sulphur or realgar; Vu [10]: common in colourless plates, up to 5 mm or white covers with sulphur and salammoniac in low-temperature fumaroles. Exploited in the past as the raw material. **Metaborite** and **clinometaborite**, Vu [74]: with sassolite and andranosite in a medium-temperature fumarole (~250°C). **Ameghinite**, Et [38]: very rare, in macrocrystalline crusts with thenardite.

3.8. Sulphates

Together with halides sulphates are the group of minerals with the largest number of various species in fumaroles. Calcium sulphates, such as gypsum and in lesser grade anhydrite, are common and in many fumaroles very abundant. Sodium sulphate, thenardite, and K-Al sulphate, alunite, can also appear in large quantities in some types of fumaroles. Specific for sulphates is existence of often several hydrous forms related to the anhydrous ones. They possess different stability fields that depend on the humidity and temperature, and can, therefore, appear in various zones of the same fumarole. The anhydrous sulphates of fumarolic origin are generally instable and readily hydrate under atmospheric conditions (anhydrite and barite group minerals are exemptions).

Chalcocyanite, Ve [9]: fairly common in greenish to sky-blue crusts, rapidly changing to chalcanthite. **Vanthoffite**, F: main phase in a white "snow-like" compact crust on lava with thenardite, löweite, and glauberite; El: in white to greyish crusts with thenardite, anhydrite, glauberite, and other sulphates. Presumed new **mineral EN**, F: in orange spongy crust together with halite, gypsum, and a mineral from voltaite group; El: in paragenesis with presumed new

mineral EA, anhydrite, langbeinite, tamarugite, and hexahydrite. The composition and crystallography of **EN** and **EA** is confirmed by SEM-EDS and XRD. They form crusts of intermixed < 10 μm isometric grains and leaves, respectively. Presumed new **mineral EI**, El [1]: in saussage-like thin fragile hollow white or red (coloured by hematite) crusts, which easily hydrate to löweite and hexahydrite when exposed to the humid atmosphere. Composition confirmed, but crystal structure unknown. **Langbeinite**, El ([1]: mineral EB): in white crusts on scoria together with sulphates or with fluorides at temperatures from 80 to 230°C; F: With anhydrite in a glassy vesicular crust covering lava. **Manganolangbeinite**, Ve [9]: in microscopic pink tetrahedra and stalactites with thenardite and Na-K chlorides. **Steklite**, [75] El: accompanying hematite with corundum, spinel and anhydrite. Very rare. **Pyracmonite**, [76] Vu: aggregates of sub-mm colourless elongated hexagonal prismatic crystals with salammoniac and kremersite in a medium-temperature fumarole (~250°C). **Aluminopyracmonite**, Vu [77]: very rare globular aggregates of prismatic colourless crystals. **Eldfellite**, [78] El: in a frothy yellow to brown crust together with tamarugite, EN and anhydrite. Very rare. Isostructural **yavapaiite**, Vu [79]: very rare minute pink crystals in association with other Fe sulphates.

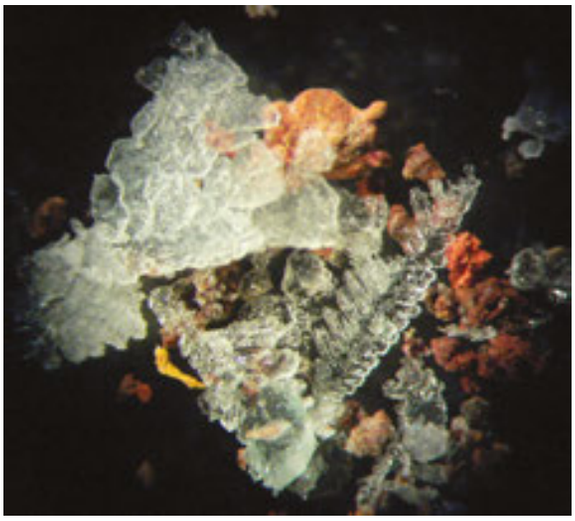

Figure 8. Dendritic aphthitalite crystals with hematite and bluish granular Cu-enriched metathenardite. Field of view 1 cm.

Thenardite is a frequent mineral in fumaroles. In Iceland, four different parageneses were observed: with gypsum, glauberite, and minor hydrous sulphates (Su, H); with metathenardite, aphthitalite, and glaserite (F, Kr, Su) with vanthoffite, anhydrite, and halite (El); with halite and minor other sulphates (A). In stalactites (Su, Ve, Et), white to lightly coloured friable microcrystalline crusts or in glass-like crusts and visible crystals when in association with aphthitalite and glaserite. The latter association includes its high-temperature polymorph **metathenardite**, stable over 271°C. Green due to Cu content, rare (F, Kr). **Aphthitalite (Figure 8)**, Ve [9], F, Kr: fairly common in millimetre size dendritic "snow flake" crystals on lava variously coloured from white to yellowish and greenish or bluish due to Cu content; Et [38]: in macrocrystalline crusts and stalactites in volcanic caves. **Glaserite**, F, Kr: in platy crystals mixed with aphthitalite. Rare. The crystal name was abandoned [80], although it is a

distinct LT phase (<150°C) in the phase system [81] with a distinct crystal structure [82]. **Palmierite**, Ve [9]: in minute hexagonal scales together with aphthitalite, ferronatrite, jarosite, and euchlorine in the "dry" fumaroles. **Mascagnite**, Ve [9]: in white crystalline crusts mixed with salammoniac, halite, and sylvite in the high-temperature fumaroles; Vu [10]: rare sub-mm colourless platy crystals with adranosite and sassolite.

Mercallite, Et [83]: in a lava tunnel; F: in fine-grained colourless crystalline aggregates on the bluish dendritic thenardite with Kröhnkite. Rare. Presumed new **mineral FB** appears with the former (F). **Therasiaite**, Vu [84]: in very rare brown equant sub-mm crystals with salammoniac. Instable.

Figure 9. Gypsum crystals. Soussaki.

Anhydrite, Su, F, El, Vu, So: common, with hematite the main constituent of the altered wall-rock, in compact to earthy materials mixed with other minerals or as separate acicular crystals; Ve [14]: rare in tabular colourless or whitish crystals. **Gypsum (Figure 9)** is one of the main fumarolic minerals in general. It forms at lower temperatures because it dehydrates already at 120–130°C. In various forms: large (> cm) crystals (So), crusts of various thicknesses from thin colourless and glassy to white or lightly coloured massive, also as efflorescence and in various associations (Su, El, CF, Ve, Et, Sa, F, N, Vu). Rare on H and M, not observed on A. **Bassanite** is stable to about 200°C. Ve [14]: in altered volcanic bombs as acicular white crystals; Su [1]: in crusts with anhydrite and gypsum; El: mixed with oskarssonite in a yellowish earthy material. Rare. Isostructural **omongwaite** [85] Su ([1]: mineral SA): in a solid white to colourless

crust on lava together with halite, anhydrite, glauberite, and other sulphates. **Glauberite**, Su,H [1] F: in small quantities accompanying thenardite and/or anhydrite. Very rare. **Barite**, M: mixed with alunite in a yellowish-white earthy crust that covers quartz crystals. Rare. **Celestite**, Et [38]: rare, in concretions in the lava caves. **Anglesite**, Ve [9]: rare, in small pale violet crystals with acicular and pseudooctahedral habit; Vu [13]: very rare in association with Bi oxy-sulphates.

Dolerophanite, Ve [9]: very rare dark brown crystals. **Antlerite**, Ve [9]: very rare, in grass-green aggregates of minute crystals as the alteration product of dolerophanite. **D'ansite** [86], A [1]: in a stalactite together with thenardite, halite, löweite, and blödite; Et [38]: in a macro-crystalline crust accompanying thenardite in a lava cave. Very rare. **D'ansite-(Mn)** [87] Ve: very rare colourless tris-tetrahedral crystals, with halite and aphthitalite. **D'ansite-(Fe)** [87] Vu: very rare aggregates of minute isometric colourless crystals with sassolite. **Aiolosite**, Vu [88]: very rare colourless acicular crystals in a medium-temperature (250°C) fumarole. **Natroalunite**, Su [1] Sa: in white-greyish crust on the inner wall of a crater, with opal, gypsum, and fluorite. **Alunite** is one of the main fumarolic minerals on Greek islands. In granular aggregates, dendritic crystals, flakes, white powdery to compact cover on lava, colourless, orange and red glassy crusts, white and yellowish botryoidal crusts, and grey cauliflower-like crusts accompanied by sulphur and alunogen and rarely by jarosite or barite, rhomboclase, and voltaite (M); constituent of the altered rock and around the fumaroles on the crater floor (N); in alteration with natroalunite accompanies sulphur in different fumaroles (Sa); in a yellow crust on lava block with halite, sylvite, gypsum, and erythrosiderite in the low-temperature fumarole (Ve [9, 14]); rare, in concretions in lava caves (Et [38]). **Natrojarosite**, El: rare in altered scoria with hematite, anhydrite, and opal with ralstonite, fluorite, and oskarssonite. **Jarosite**, El [1]: in yellow crusts together with gypsum, anhydrite, and fluorides; Ve [9]: in thin crusts with aphthitalite, euchlorine, and some chlorides; M: mixed with alunite. Rare. **Adranosite** and **adranosite-(Fe)**, Vu [89, 90]: very rare aggregates of colourless or pale yellow, respectively, acicular sub-mm crystals in medium-temperature (~250°C) fumaroles. **Euchlorine**, Ve [9]: fairly common in grass-green to emerald-green encrustations and tabular crystals together with chalcocyanite and with metavoltine. **Chlorothionite**, Ve [9]: rare greenish blue to green crusts. **Linarite**, Ve [9]: rare microscopic crystals in gypsum. **Balićžunićite** [13] and **leguernite** [91]: in cavities of a sample taken from the high-temperature fumarole (T = 600°C) in minute transparent prismatic crystals in association with anglesite and in the vicinity of sulphosalt formation. Very rare.

Kieserite, Su [1]: very rare, in association with halite, kainite, löweite, and pentahydrite in stalactites in a lava tube; Et [38]: very rare in stalactites in a lava cave. **Rozenite**, So [73]: the main mineral in white efflorescences. **Chalcanthite**, Ve [9, 14]: rare sky-blue granular masses or crusts, a product of alteration of primary fumarolic Cu minerals. **Pentahydrite**, F: very rare white sublimate on volcanic ash together with halite and **hexahydrite**: in a spongy yellowish crust with tamarugite and kainite (F); a hydration product of mineral EI and in a white crust with löweite and anhydrite (El); rare constituent of concretions in association with thenardite in lava caves (Et [38]); among sublimates at the exhausts of fumarolic vents (So). **Nickelhexahydrite**, So [73]: trace amount in a sample with römerite. **Römerite**, So [73]: the main mineral

in green efflorescences. **Coquimbite**, So: rare in a grey earthy mass mixed with gypsum, anhydrite rhomboclase, and voltaite; Sa: with rhomboclase and tamarugite accompanying alunogen. **Halotrichite:** fairly common silky white needles (CF [PSCF], N). Characteristic is the "daisy" form: halotrichite "petals" growing on the core of globular yellow core of rhomboclase (N) or presumably coquimbite [15](**Figure 10**). **Pickeringite**, CF [15]: in thick wool-like aggregates of needle-like white crystals on the wall of a cave; Et (ferroan) [83]: in an eruptive fracture (*T* around 100°C) and on the rim of the NE crater (*T* 300–400°C). **Meta-alunogen**, Et [38]: with thenardite in stalactites in a lava cave; N: in colourless platy dendritic crystals together with alunogen, tamarugite, and voltaite on the floor of the crater. **Alunogen**, Ve [9, 14]: with kalinite and as silky fibrous masses in low-temperature fumaroles; M: accompanying alunite; Sa: alternating with alunite and natroalunite as the main mineral in crusts covered by sulphur crystals; N: around the fumaroles on the crater floor. **Mirabilite**, Su [1]: in a colourless crust with thenardite in a lava tube; Ve [9]: forming from solutions and by recrystallization of fumarolic salts; Et [38]: stalagmites in a lava cave. **Campostriniite**, [92] Vu: very rare white prismatic micrometre crystals, with adranosite, sassolite, and other Bi minerals.

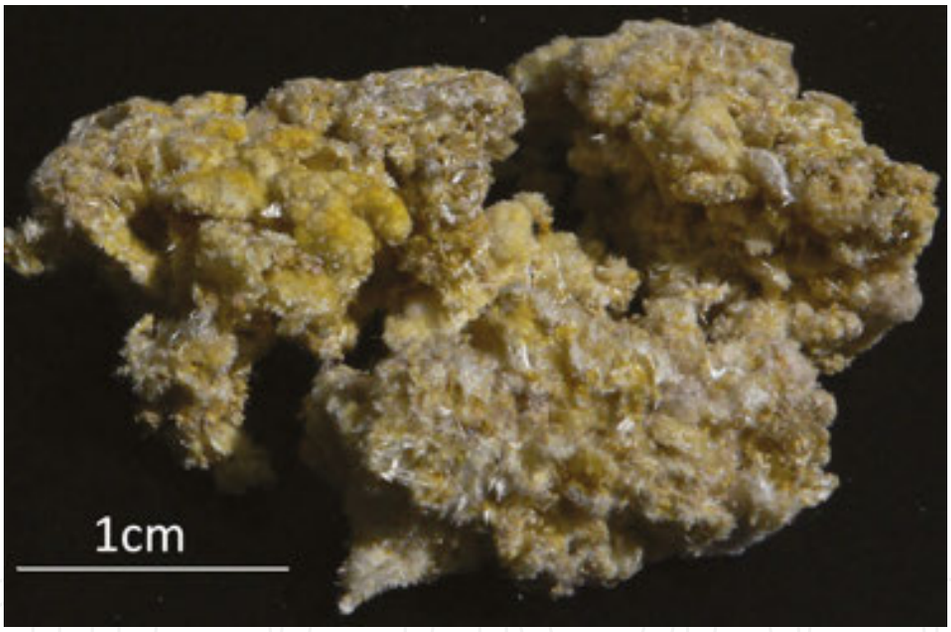

Figure 10. Yellow globules of rhomboclase with acicular halotrichite, Nisyros.

Rhomboclase, So: rare constituent of the earthy mass with gypsum, anhydrite, coquimbite, and voltaite; M: accompanying alunite; Sa: accompanying alunogen together with coquimbite and tamarugite; N: microscopic yellow globular aggregates associated with silky needles and plates of halotrichite. **Voltaite** is of a dark-green or blue to black colour due to its content of mixed-valence iron. Ve [9, 14]: rare granular aggregates of cubic crystals in the low-temperature fumarole; CF [15]: rare black lustrous crystals mixed with halotrichite; So: rare part of a grey earthy mass; M: very rare together with alunite, alunogen, rhomboclase, and pyrite; N: in granular aggregates on the crater floor with tamarugite, alunogen, and meta-alunogen. A light-coloured mineral from the voltaite group is observed in H and F samples but not

characterized in detail. **Löweite**, Su [1]: rare, in stalactites together with halite and mineral SH or Mg sulphates; A [11]: with other Na-Mg sulphates in a stalactite; El: a hydration product of mineral EI. **Eugsterite** [93] Su [1]: rare, in a soft white-to-yellow crust containing also glauberite, anhydrite, gypsum, thenardite, and Blödite. **Hydroglauberite** [94] H [1]: component of a yellow-whitish crust on lava together with thenardite and glauberite. **Syngenite**, Ve [14]: rare transparent minute tabular crystals; Et [38]: very rare, with thenardite in stalactites in a lava cave. **Kröhnkite**, F,Kr: rare, in bluish dendritic crystalline crusts with aphthitalite, glaserite, metathenardite, and thenardite. **Ferrinatrite**, Ve [9]: very rare thin fibres with adamantine lustre with aphthitalite and palmierite. **Cyanochroite**, Ve [9]: rare pale blue crystalline crusts.

Blödite, Su [1]: rare, mixed with Na-Ca sulphates and halite in stalactites and soft white-yellowish crusts; A [1]: rare, in a stalactite together with other Na-Mg sulphates; El: very rare hydration product of mineral EI; Et [38]: rare in concretions, stalactites, and macrocrystalline crusts, primarily with thenardite in lava caves. **Polyhalite**, Su [1]: very rare, in a solid white to colourless crust made of halite, anhydrite, and other sulphates; Et [38]: very rare in polycrystalline aggregates with hematite and tenorite in a lava cave. **Tamarugite**, El [1]: rare, accompanies minerals EN and EA, most probably as their hydration product and also accompanying eldfellite; F: very rare in a yellowish spongy crust with a smooth glassy surface together with hexahydrite and kainite; Sa: rare, together with alunite, alunogen, rhomboclase, and coquimbite; N: on the crater floor together with voltaite, alunogen, and meta-alunogen. **Picromerite**, Ve [9, 14]: in white to colourless crusts of elongated minute crystals; Et [38]: very rare, in concretional crusts in a lava cave. **Metavoltine**, Ve [9, 14]: in thin yellow crusts of tabular hexagonal crystals associated with euchlorine. **Kalinite** [95] Ve [9]: rare white crusts in the sulfurous fumaroles. **Alum-(K)**, Ve [14]: rare whitish crusts or octahedral to cuboctahedral crystals in medium-temperature fumarole. **Kainite**, Su [1]: rare white to colourless crusts and stalactites in mixture with other Mg, Ca, and Na sulphates; A [11]: rare, in a stalactite with thenardite and halite; F: rare, in a spongy crust with tamarugite and hexahydrite. Presumed new **mineral SH**, Su [1]: rare, in a colourless to white crust with halite, anhydrite, glauberite, kainite, omongwaite, and polyhalite and in stalactites with halite and löweite. **Chessexite** [96] El [1]: rare, in white crusts with gypsum and ralstonite at 80–100°C.

3.9. Other minerals

Chlorapatite and **mimetite** are isostructural. The former was identified in a stalactite accompanying thenardite in a lava cave (Et [38]). The latter and **phoenicochroite** accompany parascandolaite (Ve [47]).

4. European fumaroles

4.1. Icelandic volcanoes

Iceland is one of the most active terrestrial volcanic regions, with eruption frequencies of ≥20 events per century. It is also one of the most productive with magma output rates of ~8 km^3

per century in historic time [97]. Volcanism in Iceland is caused by the interaction of the Mid-Atlantic Ridge and the Iceland mantle plume. This volcanism can be traced back to the opening of the North Atlantic at 61 Ma as evidenced by massive volcanism in East Greenland, Ireland, Scotland, and the Faroe Islands. The oldest volcanic rocks exposed in Iceland are about 16 Ma [98]. During Late-Pleistocene and Holocene times, some 41 volcanic systems have been active in Iceland and its insular shelf. They are confined to volcanic zones, which are either rift zones or non-rifting flank zones. Volcanic systems in the rift zones produce rocks belonging to the tholeiitic series, while rocks of the mildly alkalic and transitional alkalic series are confined to the flank zones [99]. The majority of volcanic rocks are basalts, but significant amounts of silicic and intermediate rocks have also been produced. Encrustations have been studied from the products of seven eruptions in five volcanic systems in Iceland (**Figure 11**).

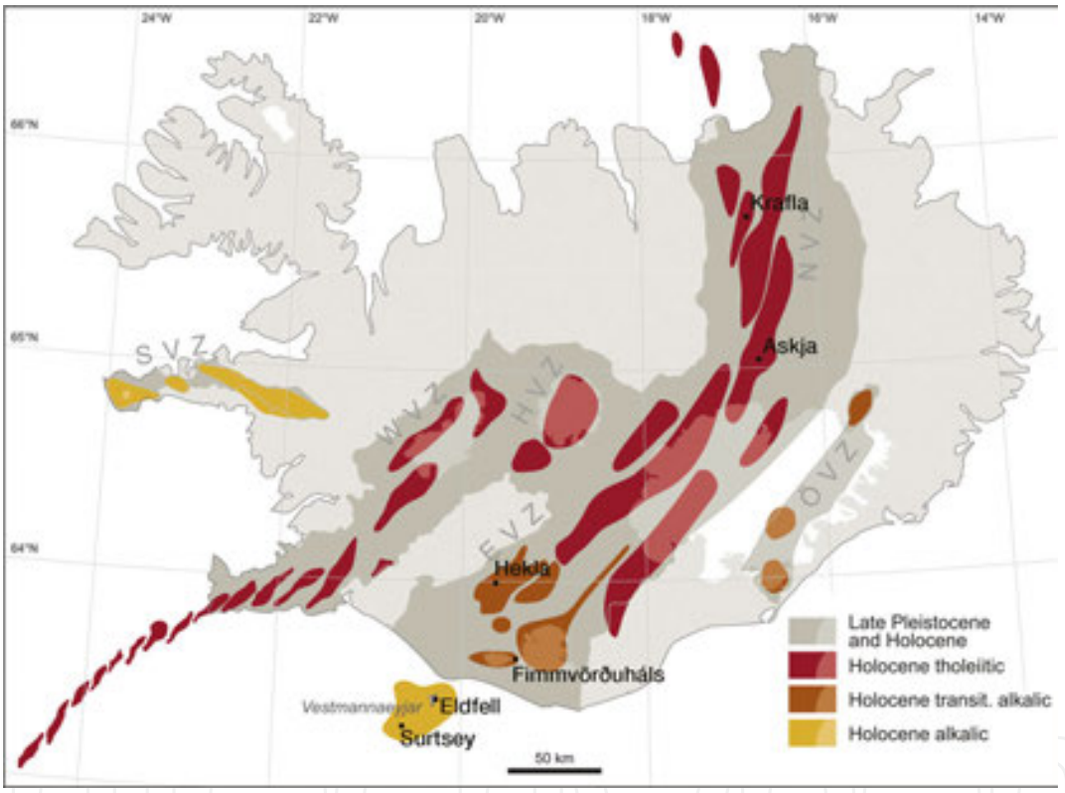

Figure 11. The volcanic systems of Iceland with the locations of investigated volcanoes.

4.1.1. The Vestmannaeyjar volcanic system

The Vestmannaeyjar archipelago represents the southernmost volcanic system in the eastern volcanic zone of Iceland. It is a partly submarine system-producing basaltic to intermediate rocks of the alkalic series. Encrustation samples from two separate eruptions were examined, the 1963–1967 Surtsey eruption and the 1973 Eldfell eruption.

The 1963–1967 Surtsey eruption. Surtsey is the south-westernmost island of the Vestmannaeyjar archipelago. It was constructed from the sea floor in a volcanic eruption occurring from

http://dx.doi.org/10.5772/64129

1963 to 1967 [100–102]. During the hydromagmatic explosive submarine phase of the eruption, from November 14, 1963 to April 4, 1964, alkali basalt tephra formed two crescent-shaped cones which merged. The eruption then evolved into an effusive alkali basalt lava phase which lasted until June 5, 1967. Two lava shields were formed with a thickness of 70–100 m. However, individual lava flow units are thin, usually only a few metres thick. The eruptive temperature of the lava was about 1140–1180°C. It is estimated that the total output of the 1963–1967 Surtsey eruption was 1.1 km^3 of basalt tephra and lava [102].

The surface encrustations on Surtsey were mainly deposited in two types of environments, as sublimates deposited directly from a gaseous state on lava and scoria at relatively high temperatures, and in a vapour-dominated system in lava craters and shallow lava caves, where steam emanation was vigorous [103]. Encrustation samples were collected in 13 expeditions from 1965 to 1998 [1]. One can recognize the following main mineral associations: 1. gypsum with thenardite, calcite, and fluorite; 2. halite with anhydrite, glauberite, thenardite, and Na-K-Mg hydrous sulphates; 3. ralstonite with other fluorides (**Figure 12**).

Figure 12. Surface encrustations on Surtsey in 1967. Photograph by H Bárðarson.

The 1973 Eldfell eruption. The Eldfell volcano is situated on Heimaey, the largest and the only inhabited island of the Vestmannaeyjar archipelago. The Eldfell eruption started on January

23, 1973, on a 1.5-km-long fissure, producing lava along its entire length. Eruptive activity quickly concentrated at the central part of the fissure and a scoria cone, Eldfell, was built up, reaching a height of 245 m asl. [104]. The Eldfell eruption ended on June 26, 1973. The magma was of hawaiite-mugearite composition [105]. At the end of the eruption, the lava covered 3.2 km^2, and the total output of lava and scoria was estimated to be 0.25 km^3 [106]. The Eldfell lava reaches a thickness of about 110 m at the eastern side of Eldfell, and large sections of the lava are 40–60 m thick. The eruptive temperature of the lava was 1030°C.

The Eldfell magma was more evolved than the magma erupted at Surtsey and as a result released a larger amount of volatiles. After the cessation of the Eldfell eruption, the extrusives and the feeder dikes have continued to release a considerable amount of gases, especially at the Eldfell scoria cone. The Eldfell lava is blocky, although large parts of it are covered with an apron of scoria. Early on, volcanic gases formed extensive encrustations on the surface of the lava and the first encrustations were already collected in February 1973 [39]. The lava encrustations on Eldfell were deposited directly as sublimates from a gaseous phase discharged from the cooling lava at a range of temperatures. Due to its thickness, the lava has been cooling down at a considerably slower rate than on Surtsey. The Eldfell crater is made up of coarse scoria mixed with volcanic bombs and lava fragments. When the crater was visited in June 2012, a narrow section of the crater rim was still very hot, reaching maximum temperatures of 290°C at 15 cm depth. Encrustation specimens were collected on the lava in 1973 and 1975, and at Eldfell crater between 1988 and 1995, and in 2009, all from the areas that were not affected by the cooling operations undertaken on the island during the eruption. The observed mineral associations are as follows: (1) (early) salammoniac, cryptohalite, gypsum, jarosite; (2) anhydrite, bassanite, gypsum; (3) anhydrite with ralstonite (later oskarssonite), jakobssonite and other fluorides; (4) anhydrite with Na-K-Al-Mg anhydrous and hydrous sulphates and (5) (late) anhydrite, hematite, corundum, anatase, opal/cristobalite.

4.1.2. The Eyjafjallajökull volcanic system

The Eyjafjallajökull volcanic system is located in the southern part of the eastern volcanic zone. It produces rocks belonging to the transitional alkalic series and consists of a ridge-shaped central volcano elongated E-W, reaching an altitude of 1651 m. It has a large summit crater flanked by mainly E-W-oriented eruptive fissures.

The 2010 Fimmvörðuháls eruption. Two connected eruptions occurred at Eyjafjallajökull in 2010. First, a basaltic fissure eruption occurred at Fimmvörðuháls on the eastern flank of the volcano. It started on March 20 and ended on April 12. Two days later, on April 14, an explosive eruption started in the summit crater of Eyjafjallajökull, which lasted until May 22nd [107]. The magma erupted at Fimmvörðuháls was a porphyritic transitional basalt, the majority of which solidified as aa-type lava, in addition to two scoria cones. The same type of basalt was involved in the explosive eruption at Eyjafjallajökull, where it was mixed with rhyolite, forming benmoreite and trachyte [108], much of which was dispersed as very fine-grained ash.

Encrustations were sampled at Fimmvörðuháls during the eruption, and at three separate times in the following months of 2010, and once in 2011. Very high gas temperatures (up to 800°C) were recorded during sampling. Volcanic ash from the Eyjafjallajökull eruption was

http://dx.doi.org/10.5772/64129

cemented into a crust on the hot surfaces of craters and lava. This provided favourable conditions for the formation and preservation of volcanogenic encrustations beneath the crust. During the eruption, thin white coatings were observed on the fresh lava. Such coatings also appeared on samples collected while hot. The coatings were found to be thenardite, a readily soluble mineral that is quickly washed away [109]. The mineral associations determined through the analysis of samples are as follows: (1) halite and sulphates (Na-K-Mg-Ca-Al) and (2) ralstonite with other fluorides (**Figure 13**).

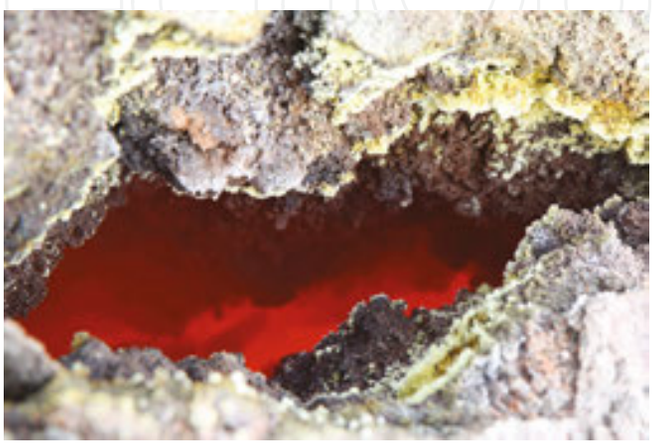

Figure 13. Formation of fumarolic minerals at 575°C in a fissure on the main scoria crater on Fimmvörðuháls about 2 months after the eruption.

4.1.3. The Hekla volcanic system

The Hekla central volcano is one of the most active volcanoes in Iceland, with more than 18 eruptions recorded in historical time. It is the production centre of the Hekla volcanic system in south Iceland. It produces basaltic to intermediate rocks of the transitional alkalic series and intermediate to silicic rocks belonging to the tholeiitic series.

The 1947–1948 Hekla eruption occurred solely within the top fissure (Heklugjá) of the volcano. The eruption started on March 29, 1947 and lasted until April 21, 1948. About 0.2 km^3 of tephra was produced during the plinian phase of the eruption. Lava covered 40 km^2 and its volume was about 0.8 km^3 [110]. The chemical composition of the extrusives changed from transitional mugearite at the beginning of the eruption, to transitional hawaiite at the end. A large amount of gas and vapour emanated from the craters, especially Axlargígur at the SW shoulder of the volcano. The encrustation samples from the 1947–1948 Hekla eruption were collected from five localities during 1947–1952. Encrustations have been observed in many of the eruptions of Hekla. For example, Schythe reports large deposits of encrustations at the craters which erupted in 1845–1846 [111].

The 1991 Hekla eruption started on January 17 with a short-lived plinian phase that was accompanied with an effusive lava phase [112]. After two days of eruption, the volcanic activity was mainly restricted to a single fissure trending east-southeast from the top of the mountain. The eruption came to an end on March 11, 1991. The 1991 Hekla extrusives are transitional

mugearite [99]. On flat ground, the lava is of a block lava type; however, on the slopes of the mountain, it is mainly of an aa type. The lava has commonly a thickness of only 4-8 m on flat ground and covers about 23 km^2. The main crater is made up of coarse scoria mixed with volcanic bombs [112]. The total amount of tephra and lava produced is estimated to be 0.15 km^3. A considerable amount of volcanic gases and vapour was released during the eruption. Pollution of groundwater and rivers around the volcano was observed already a few days after the onset of the eruption, by the rise of concentration of fluorine, carbonate, sulphate, and other dissolved solids. The average content of soluble fluorine from tephra formed on January 17 was 1600 ppm [112]. Two lava surface localities and one lava cave were visited in January and March 1991. The most prolific area with respect to encrustations was on the eruption fissure above the main crater at 1105 m asl. The lavas, the main crater and the linear eruption fissure of the 1991 Hekla eruption cooled down to ambient temperatures at the surface in less than 10 years. The surface encrustations at Hekla were mainly deposited in two types of environments, as sublimates deposited directly from a gaseous state at relatively high temperatures on lava and scoria at the linear eruption fissure, and in a vapour-dominated system in the shallow lava cave where steam emanation was vigorous.

The observed mineral associations in fumaroles are as follows: (1) (early) salammoniac, cryptohalite, gypsum, sulphur; (2) ralstonite with jakobssonite and other alumino- and silicofluorides and (3) thenardite, anhydrite or gypsum, glauberite.

4.1.4. The Askja volcanic system

The Askja volcanic system is located in the Northern Volcanic Zone in the central highland of Iceland. It consists of a central volcano with nested calderas bisected by a volcanic fissure swarm. The youngest caldera was formed following a plinian eruption in 1875. The system produces mainly tholeiitic basalts, with minor rhyolite, dacite and hybrid intermediate rocks.

The 1961 Askja eruption occurred within the large Askja caldera. It was preceded by the formation of big solfataras on a N-S line along the eastern caldera wall of Askja, about 10 days before the eruption [113]. The volcanic eruption started along a fissure northwest of the solfatara area on October 26 and lasted until November 28 [114]. It was a small eruption, only producing about 0.1 km^3 of tholeiitic basalt lava. The lava, Vikrahraun, covered 11 km^2 and large parts of it are estimated to be only few meters in thickness.

Temperatures of 420°C were still measured at a depth of 20 cm at the crater in June 1962 [113]; however, in August 1962, all soluble salts had been washed away and, apparently, no new encrustations were being formed. Encrustations formed both at the lava surface and in caves but were apparently not widespread [115]. Óskarsson [39] studied samples collected in June 1962 and found encrustations of sulfur, sal ammoniac and an NH-Fe-Cl-compound at surface, and stalactites of metathenardite in lava caves. The 1961 Askja samples available to us, all of which were presumably collected during the summer of 1962, derive from two shallow lava caves. The observed mineral associations are as follows: (1) thenardite with halite and Na-Mg-K (chloro)sulphates and (2) salammoniac.

http://dx.doi.org/10.5772/64129

4.1.5. The Krafla volcanic system

The Krafla volcanic system is located in the northern part of the northern volcanic zone. It consists of a central volcano with rhyolite formations around the rim of a caldera. A volcanic fissure swarm bisects the central volcano. The rocks belong to the tholeiitic series ranging from olivine tholeiites to rhyolites.

The 1980 Krafla eruption. The Krafla fires were a major episode of rifting and volcanism in 1975–1984 [116]. The first years were dominated by rifting, dike injections, and minor eruptions. Five larger eruptions occurred in 1980–1984. The 1980 Krafla eruption started on July 11 on several discontinuous fissures on a 4 km long line. After the first day, it concentrated on the northernmost crater where the eruption continued until July 18. The tholeiitic basalt lava covered 5.3 km^2 and the volume is estimated to be 0.02 km^3. Encrustations were collected from lava surfaces on July 30, 1980. The observed mineral associations are as follows: (1) sulphur, salammoniac; (2) thenardite with aphthitalite and (3) ralstonite with other fluorides.

4.2. Italian volcanoes

Italy is one of the most volcanically active countries in Europe. Its recent and active volcanism is mainly connected with the convergence of the Eurasian and the African plate and the extension induced by the formation of the Tyrrhenian basin, which produced volcanism along the Tyrrhenian Sea, in Sicily and Sicily Channel, and on the Tyrrhenian Sea floor. This Plio-Quaternary magmatism exhibits an extremely variable composition and permits to distinguish various magmatic provinces, which differ in major and/or trace elements and/or isotopic compositions. The most important Italian localities showing a fumarolic activity belong to the Neapolitan area (Mt.Vesuvius and Campi Flegrei), to the Aeolian Arc (La Fossa Crater at Vulcano) and to the Sicily Province (Mt. Etna). In addition to these, a number of interesting areas with actual hydrothermal activity are present in Italy, but they have not been considered in this paper because nowadays they do not produce sublimates (**Figure 14**).

Figure 14. Map of the SE Tyrrhenian Sea with locations of volcanoes and fumarolic fields.

4.2.1. The Campanian Plain

The Neapolitan Province is located in the Campania Region, along the Tyrrhenian coastline, in one of the most densely populated active volcanic areas of the Earth. The geology of the area is prevalently represented by volcanics erupted from the Upper Pleistocene to present by Mt. Somma-Vesuvius on the east, by Ischia and Campi Flegrei volcanic fields on the west and by different ignimbrite eruptions (Campanian Ignimbrites) connected to fissural volcanism along fractures activated in the Campanian Plain. Campanian Plain is a waste graben bordered by Mesozoic carbonate platforms, which began to form in Late Pliocene but largely developed in Quaternary times. Its origin is related to the counter-clockwise rotation of the Italian Peninsula and the contemporaneous opening of the Tyrrhenian Sea, which generated a stretching and thinning of the continental crust accompanied by the consequent subsidence of the carbonate platform along most of the Tyrrhenian coast. The formation of the Campanian Plain was accompanied by the uplift of the central part of the Southern Appennines, in a regional stress regime generating NW-SE and NE-SW-trending faults and establishing the ideal conditions for magma to form and rise to the surface. With the exception of oldest volcanic rocks with calc-alkaline composition, erupted magmas younger than 400 ka are alkaline, with high potassium compositions erupted only at Vesuvius [117].

4.2.2. The Phlegrean Fields

Figure 15. As-sulphide fumarole at Pozzuoli, Campi Flegrei. Photograph by courtesy of Fabrizio Reale.

The Phlegrean Fields (Campi Flegrei: “The Burning Plain") are an area of active volcanism located about 25 km west of Vesuvius and 5 km west-southwest of Naples and consists of a large caldera formed about 35,000 years ago with the eruption of 80 km^3 of ash (the Campanian Tuff). The caldera is about 12 km in diameter and includes a series of mostly monogenetic pyroclastic vents. After the caldera formation, with a progressive decrease in volume of the emitted products, the eruptive centres migrated towards the centre of the caldera. There were two historic eruptions in the area. The 1198 phreatic eruption was at Solfatara, a pyroclastic cone formed about 4000 years ago and still in a fumarolic stage. The last one in 1538 produced

http://dx.doi.org/10.5772/64129

the new pyroclastic cone of Monte Nuovo. It was explosive and generated pyroclastic flows, but also produced a lava lake and lava flows. After that, the Phlegrean area is characterized by fumarolic activity and periodic episodes of unrest involving seismic activity and slow ground motion (bradyseism) with uplifts. Spectacular fumaroles, with temperatures rising to 160°C, are mainly located at the Solfatara cone, but occur also along active fractures throughout the area both on land and in the Gulf of Pozzuoli. They belong to a widespread geothermal system, which is characterized by a geothermal gradient of up to 170°/km, numerous superimposed aquifers, and a zoning typical of hydrothermal mineral deposition [118]. The predominance of magmatic volatiles over the meteoric water in the volcanic fluids is suggested by isotopic compositions, as well as by the modelling of the fluxes of CO_2 and S. The mineralogy of Solfatara is generally characterized by sulphur and a sulphate paragenesis (alunite and alunogen with other sulphates) [119]. At La Bocca Grande vent, where the vent temperature reaches 160°C, arsenic sulfides (realgar and pararealgar) are deposited [120] (**Figure 15**).

4.2.3. Mt. Somma-Vesuvius

The present Somma-Vesuvius is a moderate size composite central volcano rising more than 1200 m asl. The activity of Monte Somma has been characterized by a series of sub-Plinian and Plinian eruptions alternating with long quiescent periods lasting from centuries to millennia, followed by periods of semipersistent activity characterized by lava effusions and low-energy explosive eruptions in the past 4 kyr. The Plinian AD 79 eruption [121] broke a long period of quiescence and represented one of better-known devastating events in the Mt. Vesuvius history. The recent Vesuvius cone has grown within the oldest Mt. Somma caldera possibly after this eruption. After it, the volcano featured two sub-plinian events in AD 472 and 1631 [121]. Throughout the following centuries, Vesuvius activity was characterized by periods of open-conduit activity with the alternating strombolian activity with violent eruptions. The eruption of 1906 is the largest explosive eruption of the twentieth century. The climax of the eruption was reached on the April 7th, when impressive lava fountains, accompanied by earthquakes, rose from the crater. At the end of the eruption, the top of the cone was truncated to form a vast crater. After this explosive event, the Vesuvius area was characterized by quiescent periods alternated by prolonged volcanic activity, effusions of lava and low energy explosions. The last eruption occurred in March 1944.

Mt. Vesuvius is presently affected by relatively low level volcanic-hydrothermal activity, which is mainly characterized by the following: (a) widespread fumarolic emissions that are accompanied by diffuse soil CO_2 degassing in the crater area [122]; (b) CO_2-rich groundwaters along the southern flank of Vesuvius and in the adjacent plain and (c) seismic activity with epicentres clustered inside the crater [123]. Fumarolic fluids discharging by the crater rim fumaroles are of relatively low temperatures (<75°C) and are mainly composed of atmospheric components. Fumaroles from the crater bottom have H_2O and CO_2 as the major components, followed by H_2, H_2S, N_2, CH_4, CO, and He (in order of decreasing content), and discharge temperature of about 95°C [123]. CH_4 and NH_3 contents suggest that the origin of these fluids could be from a high-temperature hydrothermal system located below the Vesuvius' crater [122]. Lacroix classified older Vesuvian fumaroles in four different types [9]: (1) HT (>300°C)

with halite, sylvite, thenardite, Na-K carbonates, aphthitalite, sulphides, Cu-oxide and chlorides (alteration); (2) ("acid", *T*=300–100°C) with Mg-Fe-Al chlorides, sulphur, and realgar; (3) (around 300°C) containing salammoniac with ammonium sulphate and fluoride and (4) (sulphurous, LT around 100°C) with sulphur, gypsum, sassolite, K-Al-Fe sulphates, opal.

4.2.4. Vulcano Island

Vulcano is the southernmost of the seven islands that form the Aeolian archipelago. Its activity dates back about 120 Ka. The four main eruptive centres of the island (Vulcano Primordiale, Lentia, La Fossa cone, and Vulcanello) are formed by a progressive migration of the volcanic activity from SSE to NNW. In the middle of La Fossa caldera sits La Fossa cone, the active volcanic centre of the island, which formed during the last 5.5 ka through recurrent hydro-magmatic to volcanic explosive phases [124]. Since its last eruption in 1888–1890, Vulcano has remained in a fumarolic stage of varying intensity with shallow seismicity. Presently, active fumarole fields are concentrated in the northern section of the La Fossa crater and in the neighbourhood of the coast at Baia di Levante. The former show high variability in temperature and fluid compositions as a function of the volcanic activity, the latter are typical hydrothermal emissions.

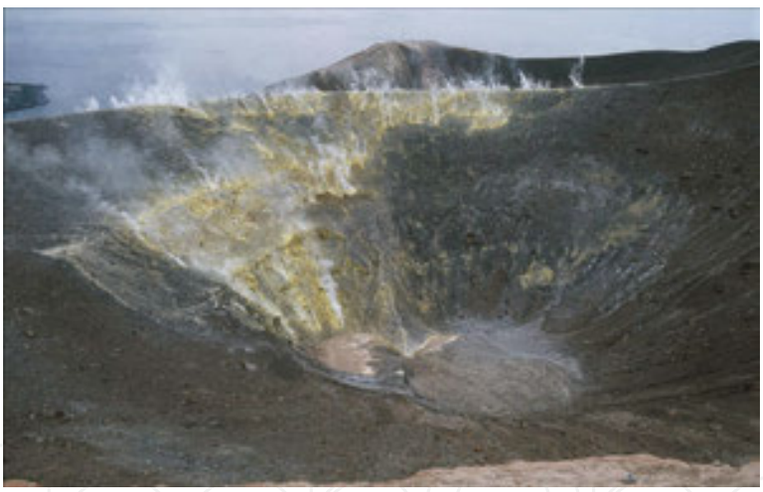

Figure 16. Fumaroles on La Fossa Crater, Vulcano.

Over the last two decades, several models were proposed to explain the genesis of the Vulcano fumarole fluids, each of them involving the presence of a deep and a shallow component in the gas phase. Compositionally, the crater fumaroles are rich in CO_2 as the main component and have significant concentrations of HCl, SO_2, H_2S, HF, and CO [125]. The diffuse emissions at Baia di Levante are more typical of hydrothermal fluids, with higher CH_4 and H_2S contents than the crater fumaroles, lower CO concentrations, and no measurable amount of SO_2 [126]. Strong variations of the chemicophysical features of the gas output at the crater have been observed periodically. During these so-called "crisis", the crater fumaroles demonstrated a substantial increase in temperature from the usual range between 330 and 400°C and in the magmatic component of the total gas flux. The interest in the collection and analysis of the

http://dx.doi.org/10.5772/64129

fumarolic minerals especially increased during the last thermal crisis, which started in 1988 and reached a maximum in 1993. A systematic research was started, supported by the Italian National Group of Volcanology. This led to the discovery of a large variety of rare phases and new minerals [8, 12, 13, 26–29, 31–34, 40, 49, 55, 66, 90, 91]. La Fossa crater became a mineralogical attraction and the large number of already described minerals from the locality [10] increases constantly making it one of the most prolific type locality in the world. The fumarolic mineral association observed on La Fossa Crater are (1) (LT + MT) sulphur, borates, borosilicates, sulphates (mainly hydrous, only in oxidizing conditions), halogenides and sulfohalogenides and (2) (HT >400–450°C) sulphides, sulphosalts, sulfochlorides (reducing conditions); anhydrous sulfates (oxidizing conditions) (**Figure 16**).

4.2.5. Mt. Etna

Mount Etna is one of the largest European volcanoes, world famous for its spectacular and frequent eruptions. Its main feature is the voluminous lava emission, occasionally associated with explosive activity from its four summit craters. Mt. Etna is a basaltic composite apparatus, with a basal diameter of 40 km and 3350 m of altitude, situated on the eastern border of Sicily. The Etnean volcanism is still not definitely understood in its geological context. Mt Etna is situated on the crossing of important regional fault systems trending NW-SE, NE-SW, and WSW-ESE and this probably facilitates the uprise of magma in this place. There is some evidence that Etna is but the most recent manifestation of volcanism fed from a very long-lived mantle source, having caused numerous earlier phases of mafic volcanism in the Monti Iblei, SE Sicily, from the late Triassic to the early Pleistocene. Mt. Etna has erupted many times in historical time and presently is constantly active with spectacular summit and flank eruptions, interspersed by periods of intermittent activity. The recent volcanic activity has been characterized by almost continuous summit eruptions of effusive and moderate explosive activity. Its most powerful historical eruption occurred in 122 BC [127]. This plinian summit eruption produced a large volume of pyroclastics (ash and lapilli), which fell in a sector on the southeast flank of the volcano, causing devastation in the city of Catania. Presently, the frequent eruptive activity heavily affects the morphology of the summit area that consists of a central crater (Voragine) surrounded by three active cones (Bocca Nuova, NE Crater, and SE Crater) and is cut by N-S-oriented fracture system, mainly related to the extensional stress produced by magma ascent [128]. From the four active craters in historical times, a large number of summit and flank eruptions have occurred [129] producing numerous composite lava fields and more than 300 scoria and spatter cones. The chemical composition of magmas produced in historical times is rather uniform, ranging from alkali basalt to basic mugearite.

The fumarolic activity at the crater area of Mt. Etna is variable and largely influenced by the activity of the volcano, which is continuous and changes frequently. Consequently, as the morphology of the summit area undergoes significant variations over time, also the localization and amplitude of gas discharging and temperature of fumaroles change. Generally, the fumaroles are aligned along dynamic fractures produced by extensional stress phenomena, but also around hornitos. Intense fumarolic activity is often present due to residual degassing during the cooling of erupted lava. The most of the gas discharging is from the surface of lava

flows, but it also happens in the inner parts of volcanic lava tubes and caves in which the cooling of the gases often produces interesting deposition of sublimates and encrustations. After exsolving from magmas, the gases ascend along rock fractures sometimes reaching directly the surface (high-temperature fumarole). In other cases (low-temperature fumarole), they interact with peripheral hydrothermal systems and surficial acquifers, undergo contamination and change their pristine composition [130]. The observed main mineral associations are as follows: (1) (surface, HT) thenardite, halite and sylvine; (2) (surface, LT) sulphur, salammoniac, hydrous sulphates and (3) (in caves) halite, sylvite with thenardite, and hydrous sulphates.

4.3. Greek volcanoes

4.3.1. The Aegean (Hellenic) active volcanic arc

The Aegean volcanic arc is one of the tectonically most active regions of the Mediterranean area, extending from the mainland of Greece through the volcanic centers of Soussaki, Aegina, Methana, Poros, Milos, Santorini, Kos, Yali, and Nisyros, to the Bodrum peninsula in Turkey. In that area, the eastern Mediteranian lithosphere subducts under the Aegean and the Aegean microplate overrides the eastern Mediterranean [131]. The volcanism started 3.5 Ma ago and is still continued up today in the form of post-magmatic activity [132–135]. The Pliocene-Quaternary volcanic arc of the Aegean arose from the subduction of the African plate beneath the microplate of the Aegean-Anatolian [136] with simultaneous destruction of intermediate-Tethys oceanic crust. The Pliocene-Pleistocene volcanism in the arc of the Aegean Sea is

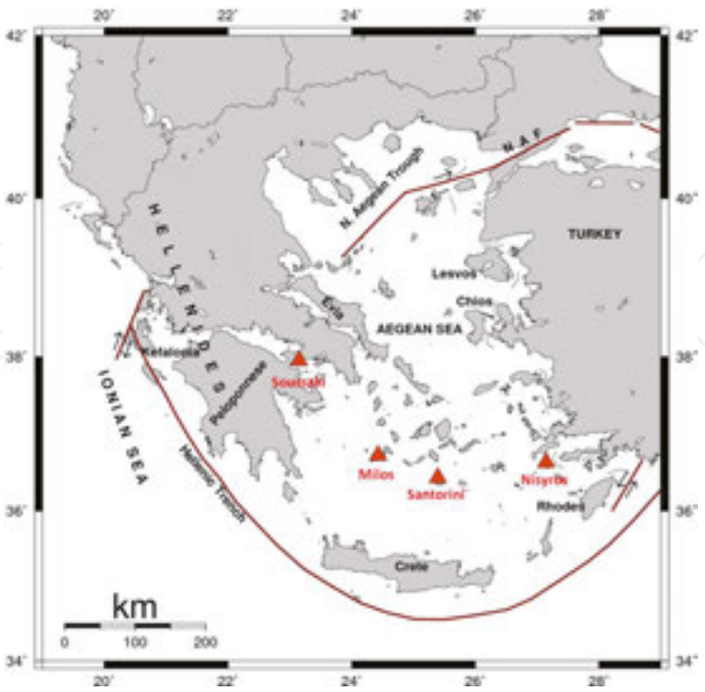

Figure 17. Map of Greece with the locations of the investigated volcanoes and fumarolic fields.

dominated by andesites and dacites, while in the central and eastern parts of the arc, the lower Quaternary volcanism is characterized by dacitic or rhyolitic composition (**Figure 17**).

4.3.2. Soussaki volcano

The Soussaki area represents the NW end of the active Aegean volcanic arc. The volcanic activity took place between 4.0 and 2.3 Ma ago. The lithological types occurring in the area are rocks of the dacitic and rhyolitic composition, remnants of the late Pliocene to Quaternary volcanic activity [132–135, 137]. Gas manifestations display typical geothermal compositions with CO_2 and water vapour as the main components and CH_4 and H_2S as minor species. The volcanic activity observed today manifests itself by emanation of warm fluids, while widespread fumarolic alteration, vapours, and warm (35–45°C) gas emissions are still observed. Reaction between the fluids and pre-existing rocks, consisting mainly of serpentinite, chert, marlstone, limestone, and subordinate rhyodacitic lava, has resulted in the formation of gypsum, sulphur, silica polymorphs, and Fe and Mg sulphates. Kaolinite, anhydrite, carbonates, and Ni, and K-Al sulfates are also present in some cases ([73], this work). The observed main mineral associations can be summarized as follows: (1) gypsum with quartz and carbonates and (2) Fe-Mg hydrous sulphates.

4.3.3. Milos Island

The Milos volcanic district is a wide volcanic archipelago comprising the islands of Milos, Kimolos, Antimilos, and Poliegos. The volcanic activity started about 5 million years ago and is now considered to be extinct. Milos Island is located at the western end of the Aegean Volcanic Arc. It is built mainly of calcalkaline volcanic rocks (tuffs, pumice flows, ignimbrites, pyroclastic flows, domes, and lava flows of andesitic-dacitic, and rhyolitic composition). The volcanic sequence is built on Miocene-Pliocene clastic and carbonate platform sediments, which unconformably overly a metamorphic basement. Following their emplacement, volcanic rocks were involved in an intense hydrothermal activity. The volcanism in the area developed with submarine activity character and was followed by a sub-aerial effusive phase. The distribution of the hydrothermal minerals derived basing on cores and cuttings from the two drill sites to a depth of about 1100 m [138] indicates the dilution of the K-, Na-, Cl-rich hydrothermal fluid of the deep reservoir by a Ca-, Mg-rich cold water at a shallower level. In some places, the hydrothermal activity is expressed by the occurrence of many hot springs (30–85°C), fumaroles (98–102°C), hot grounds (100°C at a depth of 30–40 cm) and submarine gas emissions, widespread on and around the island. Fyriplaka volcano is the expression of the most recent volcanic activity on the island and includes fumaroles, solfataras, and hot grounds. Where gas emanations are very high, the soils are altered and covered with thin layers of secondary minerals as alunite, magnesite, and sulphur.

We examined samples from the area of Amygdales and in the neighbourhood of Paleochori. The substrate rock is argillaceous, composed of SiO_2 polymorphs and kaolinite mixed with alunite, which is the dominating fumarolic mineral. The main fumarolic associations are as follows: (1) alunite with sulphur (plus quartz, opal, kaolinite) and (2) alunite and alunogen with Fe-hydrous sulphates and barite (plus sulphur, pyrite, quartz, opal, muscovite).

4.3.4. Santorini volcano

The volcanic field of Santorini consists of various islands (Thera, Therasia, Aspronisi, Palea Kameni, and Nea Kameni), the Christiania islands around 20 km to the southwest and the submerged Columbus volcano 7 km to the northeast. It is the most active part of the Aegean Volcanic Arc. Between Thera, Therasia, and Aspronisi, exists a sea-flooded caldera of about 13 km diameter. According to various geochronological data, the volcanic activity in the Santorini volcano started about 2 Ma ago. The field has had 12 major (1–10 km^3 or more of lava), and numerous minor, explosive eruptions over the last ~200 ka. A hypothesis the eruption mechanism [139] supposes a large water-filled crater, an extensional environment to facilitate downward penetration of water, and a hot silicic magma.

Figure 18. Fumarole on Nea Kameni, Santorini.

Nea Kameni fumaroles have a distinct hydrothermal nature with compositions dominated by H_2O, CO_2 and H_2 with minor H_2S, and SO_2 typically absent [140]. We investigated samples from the fumaroles at the Nea Kameni central crater. The altered rock consists of cristobalite, opal, plagioclase (around An50), gypsum, alunite or natroalunite and sporadic quartz, trydimite, hematite, and kaolinite. The sublimate is mostly sulphur that makes yellowish crusts, aggregates of isometric crystals or spear-like dendritic crystals. Hydrated sulphates are alunogen (mixed with the substrate or as thin platy crystals), rhomboclase, coquimbite, and tamarugite. Jarosite is also found in small quantities (**Figure 18**).

4.3.5. Nisyros volcano

Nisyros is the newest of the major active volcanoes of Greece, composed almost exclusively of volcanic rocks, with the oldest of them being little less than 160,000 years and the youngest

http://dx.doi.org/10.5772/64129

reaching the limits of prehistory, about 20,000 years ago. In the wider area of Nisyros at the eastern margin of the volcanic arc, the first eruptions date 3.4 million years. Since then, small or large eruptions built up Nisyros and the islets Pirgousa, Pachia, Strogyli, and Giali. None of the eruptions of the volcano recorded in historical sources produced molten rock, as they are hydrothermal and originate from the overheated steam in the underground of the island. Seawater and rainwater penetrate the rocks of the island, are heated by magma and converted to superheated steam, which exerts tremendous pressure and causes a hydrothermal explosion when overcomes the weight and consistency of the caprock. Such explosions were recorded in Nisyros in historical times. In the southern part of the caldera floor, there are traces of 20 craters, 10 of them being well preserved. The largest and most striking crater is Stephanos. The latest hydrothermal craters are concentrated in the area of Lofos (=hill), a small post-dome that largely has been destroyed by hydrothermal explosions. Here are situated six well-preserved craters, the creation of three of them being recorded in historical sources. In October or November 1871, a powerful earthquake caused the beginning of a series of hydrothermal explosions, which until 1873 created two small craters: Polyvotis and Alexandos (or Flegethron). The last recorded hydrothermal explosion in Nisyros is the one of 1887, which created the crater of Small Polyvotis. Various amounts of volcanic gases come out from the intracaldera soil area including also the main fumarolic craters of Kaminakia, Ramos, Stefanos, Lofos, and Flegethron. The gas species are H_2S, CO_2, CH_4, and CO [141–143](**Figure 19**).

Figure 19. Fumaroles in the Stephanos crater, Nisyros.

The only sublimate mineral observed at the vents at the edges of the Stefanos and Polyvotis craters is sulphur. It develops as granular aggregates or acicular spear-like crystals. On the floor of the Stefanos crater, numerous circular formations surround the "hot spots" of the fluid, vapour, and gas emanations. The central part of these formations consists of the reddish to yellowish sand formed by grains of quartz, labradoritic plagioclase, alunite, alunogen, and gypsum. They are surrounded by white rims containing dendritic crystals of alunogen and

metaalunogen. On their outer part is a blackish zone with additional voltaite and tamarugite. The outermost rim consists of aggregates of microscopic yellowish globules of rhomboclase overgrown by silky needles of halotrichite.

5. Discussion

The list of the minerals found in European fumaroles impresses by the number of different species, especially taking in account that some prolific mineral groups (like silicates and phosphates) do not contribute to the list or contribute very little. Among the European fumarole localities, Vesuvius and Vulcano stand as the two volcanoes with the richest mineralogy. This status is due to the exceptional abundance of otherwise rare elements in their emanations: Cr, Mn, Ni, Cu, B, Tl, Pb, As, Se on Vesuvius, Ba, Au, Zn, B, Tl, Sn, Pb, As, Bi, Se, Te, Br, I on Vulcano. The presence of the rare elements that form rare minerals is, however, not the only reason for the diversity of fumarole mineralogy. Although they do not contain minerals of rare elements, the three Icelandic volcanoes Surtsey, Eldfell, and Hekla each have around 30 different minerals in their fumaroles. Moreover, their dominating mineral associations are different from the main associations of both Vesuvius and Vulcano, and are differing among themselves, although all five fumarolic systems are formed by the same combination of main gaseous species (H_2O, CO_2, HCl, HF, SO_2, and H_2S). This illustrates the importance of various factors that can influence the processes and through that the mineral world of fumaroles mentioned in the introduction. The intensive parameters, composition and temperature of volcanic gases and lava, can decisively be supplemented by other factors in forming or modifying the minerals in fumaroles. We will try to examine them in the following comparison of different fumarolic systems.

In general, the fumaroles can be classified according to their temperature of formation and mineral stability. Already in the nineteenth century, Lacroix made a classification of Vesuvius fumaroles [9] after their mineralogy, reflecting the temperature of formation. He distinguished the high-temperature "dry" fumaroles characterized by the K and Na salts and also some sulphides and oxides, the medium-temperature "acid" fumaroles characterized by the chlorides of Fe, Mg, Al, and Mn, fumaroles of even lower temperature characterized by salammoniac and other ammonium minerals, and the low-temperature fumarole producing sulphuric acid and steam with sulphur and gypsum as typical minerals. We shall try to classify the fumaroles investigated in this work in three categories: (1) HT, the high temperature (>400°C), (2) MT, medium temperature (200–400°C) and (3) LT, low temperature (<200°C). The given temperature ranges are approximate. HT fumaroles appear with the eruption of the volcano and are short living after its finish. Alternatively, they can be products of temperature increase in the volcanic system not leading to eruption, but again short-lived (Vulcano). MT and LT fumaroles might be active at the same time as the HT fumaroles, but at different places in the system where fumarolic gases travelled longer and got cooled and/or diluted by the atmosphere before they come to the surface. MT fumaroles prevail in the period of recession after the paroxysm and last roughly for decades, maybe centuries, while the shallow intruded magma cools down, or the degassing surface of the magma retreats to greater depths. LT

http://dx.doi.org/10.5772/64129

fumaroles are the only ones present in the quiescence period with a deep thermal source and may transform eventually to a solfatara (mofeta), if the volcanic cycle is finished or very much prolonged.

Inspecting the mineralogy of European fumaroles, we can see that specific three (or four) minerals are typical in most cases for the HT fumaroles. These are halite, (meta) thenardite (with or without aphthitalite), and anhydrite. The mentioned four minerals are all stable to over 800°C. The fumarolic systems can be classified according to relative abundances of these minerals reflecting the Na(+K)/Ca and Cl/S proportions in the fumarolic paragenesis. In this classification, the alcalic fumaroles are those of Vesuvius (dominantly chloridic), Fimmvörðuháls and Askja (chloridic-sulphatic) and Krafla (sulphatic). The mixed alcalic-calcic are Surtsey and Etna (chloridic-sulphatic) and Hekla (sulphatic), the calcic is Eldfell (sulphatic). Outside the classification stands Vulcano, with a high-temperature association composed of sulphides/sulphosalts in combination with sulphochlorides. It can be locally expanded with an association of anhydrous sulphates where and when the atmospheric influence is large and the general reducing conditions change to oxidative.

The MT fumaroles reflect more the individual nature of each fumarolic system. First of all, the range of temperature, the relatively slow flux rates and the chemistry of fumarolic systems permit the deposition and the growth of a larger number of mineral phases, including products of reaction between gas, steam, or liquid and minerals previously formed. In addition, the often longer time of their existence and the longer and slower ascent of the fluid phase allows for a larger contribution of other influences on magmatic exhalations, that is, interaction with the wall rock and surficial fluids. Here, we can recognize the following associations: A, salammoniac in association with other ammonium minerals; B, metal chlorides (Fe-Al-Mg plus others); C, fluoride association with ralstonite as the dominating mineral, typically mixed with other aluminofluorides. Type A was registered on all recently active volcanoes except Surtsey and Fimmvörðuháls. On Eldfell and Hekla, it was forming only early following the eruption. On Vesuvius and especially Vulcano, it is a persistent feature, where the latter also demonstrates a rich variety of ammonium minerals not found on other places. The situation on Icelandic volcanoes suggests that nitrogen in the volcanic gases is one of the first species to be exhausted upon an eruptive episode. If it is true, it would mean that the shallow-degassing magmas of Vesuvius and Vulcano are constantly replenished in nitrogen or that it is there supplied from some other sources. Type B is found on Vesuvius and Vulcano. On the former, the chlorides are mixed with fluorides, on the latter with fluorides (boro- and silicofluorides), bromides and even an iodate. The type C is characteristic for a number of Icelandic volcanoes (Surtsey, Eldfell, Fimmvörðuháls, Hekla, Krafla). In Hekla fumaroles, silicofluorides appear together with aluminofluorides.

The dominating minerals in the LT fumaroles are sassolite, gypsum, alunogen, and sulphur (listed with decreasing thermal stability). The differences in thermal stability are practically of no importance in this group because all minerals form at temperatures that are around 100°C or even lower in this type of fumaroles. Here, also alunite can be named as an abundant component. It is a product of feldspar decomposition through action of sulphuric gases and solutions in solfataras and low-temperature fumaroles, together with opal, and in this respect

does not represent a simple sublimate. It is stable to around 500°C and could be a component of high-temperature fumarole as well, but the process of formation makes it a typical representative of the low-temperature one. The LT fumaroles can be categorized by the contents of the above-mentioned minerals. The sulphur dominated fumaroles are found on Nisyros, Etna, Campi Flegrei, Vesuvius, Vulcano, and Krafla. Gypsum dominated are those of Soussaki, Surtsey, Eldfell, and Hekla. Vulcano and Vesuvius have low-temperature fumaroles that contain also abundant sassolite together with sulphur and gypsum. The second type of fumaroles on Nisyros and fumaroles on Milos are dominated by alunogen, and finally, the fumaroles on Santorini have comparable amounts of sulphur, gypsum and alunogen. In all of them, various kinds of hydrous sulphates appear, which can be used as fine-tuning indicators of temperature and humidity conditions.

The classifications given above can serve a general orientation purpose and understanding of the actual conditions in the fumarolic system under investigation. They are in no way clearly delimited categories and mixing of associations is a frequent phenomenon. It can be produced as a consequence of the gradual lowering of temperature and the flux rate, but often also a simultaneous formation of closely separated minerals at quite different temperatures occurs due to the high fluctuation of conditions on a small scale at the border between the volcanic gases and the atmosphere. On Vulcano, the high-temperature anhydrous sulphates that form under the locally oxidizing conditions are found in close association with sulphides and sulphosalts formed under the reducing conditions. Our detailed investigation of fumarolic profiles on Eldfell shows that within less than 20 cm the low-temperature mineral association of fluorides changed to the high-temperature association of anhydrous sulphates. The mixed associations can also be an artefact produced by the mineral instability at atmospheric conditions, and laboratory analyses taken alone can give misleading results. Our analyses of Eldfell material showed always hydrous Mg-Al sulphates accompanying the anhydrous ones taken from the levels featuring temperatures over their stability ranges. Their formation as atmospheric hydration products was confirmed by the field observations of the deliquescent behaviour of exposed excavated samples and through laboratory analyses of freshly crushed massive ones. The caveat about the above classification is that it presents a general picture from which numerous important details have been removed in order to give as clear as possible an overview. For a full characterization of individual fumarolic systems, the details are indispensable, and this emphasizes the importance of detailed studies.

The realm of fumarolic mineralogy presents us with interesting and important still unanswered questions. For example, the seeming contradiction of the experimental results that show sulphuric species to be the ones with the fastest and earliest devolatilization from silicic melts, and the observation that sulphates and elemental sulphur are the most persistent parts of fumaroles, leads to important enquiries into the sub-surface volcanogenic sulphuric cycle (see e.g. [144]). Another interesting largely unsolved problem is the understanding of reasons why sometimes large differences in mineral compositions of seemingly similar fumarolic systems exist. During the last century, the appearance of powerful methods of research on microscale has revealed a great number of new mineral species from fumarolic samples, typically rare and exotic, and contributed to the solid state science and the general minera-

logical knowledge. We believe that the application of these methods to investigation of both minor and main components of fumaroles and integrated with research in other fields (like gas evolution and composition and gas-magma-rock interactions) can also bring answers to the most intriguing questions of the genesis and origins of particular fumaroles. Accomplishing this, they can become another important tool in the surveillance of active volcanic systems.

Acknowledgements

The authors are grateful to researchers and students with whom they collaborated in the investigations of European fumaroles: Filippo Vurro, Daniela Pinto, Donatella Mitolo, Eric Leonardsen, Sigurður S. Jónsson, Níels Óskarsson, Sigmundur Einarsson, Anna Katerinopoulou and Morten J. Jacobsen. We thank Helene Almind for the technical assistance during XRD measurements and Dora Balić Žunić for technical support during the field work and manuscript preparation. Parts of the research work were financially supported by the Danish Agency for Science Technology and Innovation and the National Group for Volcanology, Italy.

Author details

Tonči Balić-Žunić[1*], Anna Garavelli[2], Sveinn Peter Jakobsson[3], Kristjan Jonasson[3], Athanasios Katerinopoulos[4], Konstantinos Kyriakopoulos[4] and Pasquale Acquafredda[2]

*Address all correspondence to: toncib@snm.ku.dk

1 University of Copenhagen, Copenhagen, Denmark

2 University of Bari, Bari, Italy

3 Icelandic Institute of Natural History, Gardabaer, Iceland

4 University of Athens, Athens, Greece

References

[1] Jakobsson SP, Leonardsen ES, Balic-Zunic T, Jónsson SS. Encrustations from three recent volcanic eruptions in Iceland: the 1963–1967 Surtsey, the 1973 Eldfell and the 1991 Hekla eruptions. Fjölrit Náttúrufræðistofnunar (Special Publication of the Icelandic Institute of Natural History).2008;52:65 p.

[2] Ruste J. X-ray spectrometry. In: Maurice F, Meny L, Tixier R, editors. Microanalysis and Scanning Electron Microscopy. Orsay: Les Editions de Physique; 1979. pp. 215–267.

[3] Acquafredda P, Paglionico A. SEM-EDS microanalyses of microphenocrysts of Mediterranean obsidians: a preliminary approach to source discrimination. European Journal of Mineralogy. 2004;16:419–429.

[4] Pouchou JL, Pichoir F. Quantitative analysis of homogeneous or stratified microvolumes applying the model "PAP". In: Heinrich KFJ, Newbury DE, editors. Electron Probe Quantitation. New York: Plenum Press; 1991. pp. 31–75.

[5] Strunz H, Nickel EH. Strunz Mineralogical Tables. 9th ed. Stuttgart: E. Schweizerbart'sche Verlagsbuchhandlung (Nägele u. Obermiller); 2001. 870 p.

[6] Panichi U. Muthmann'scher Schwefel, auf der Insel Vulcano beobachtet. Zeitschrift für Krystallographie. 1915;54:393–394.

[7] Steudel R, editor. Elemental Sulphur and Sulphur-Rich Compounds I, Topics in Current Chemistry 230. 1st ed. Berlin, Heidelberg, New York: Springer; 2003. 166 p.

[8] Garavelli A, Mitolo D, Pinto D, Vurro F. Lucabindiite, $(K,NH_4)As_4O_6(Cl,Br)$, a new fumarole mineral from the "La Fossa" crater at Vulcano, Aeolian Islands, Italy. American Mineralogist. 2013; 98;470–477.

[9] Pelloux A. The minerals of Vesuvius. American Mineralogist. 1927;12:14–21.

[10] Campostrini I, Demartin F, Gramaccioli CM, Russo M. Vulcano: tre secoli di (Vulcano: three centuries of its mineralogy). Cremona: Ami Associazione Micromineralogica Italiana; 2011. 343 p.

[11] Fulignati P, Sbrana A. Presence of native gold and tellurium in the active high-sulfidation system of the La Fossa volcano (Vulcano, Italy). Journal of Volcanology and Geothermal Research. 1998;86:187–198.

[12] Garavelli A, Laviano R, Vurro F. Sublimate deposition from hydrothermal fluids at the Fossa crater – Vulcano, Italy. European Journal of Mineralogy. 1997;9:423–432.

[13] Pinto D, Garavelli A, Mitolo D. Balićžunićite, $Bi_2O(SO_4)_2$, a new fumarole mineral from La Fossa crater, Vulcano, Aeolian Islands, Italy. Mineralogical Magazine. 2014;78:1043–1055.

[14] Russo M. I minerali di formazione fumarolica della grande eruzione Vesuviana del 1906 (Minerals of fumarolic origin from the large 1906 eruption of Vesuvius). Istituto Nazionale di Geofisica e Vulcanologia, sezione Napoli – Osservatorio Vesuviano. Open File Report; 2006. 39 p.

[15] Parascandola A. Contributo alla mineralogia Flegrea (A contribution to the Phlegrean mineralogy). Bolletino della Società Geologica Italiana (Bulletin of the Italian Geological Society). 1951;70(3):527–532.

[16] Emelina AL, Alikhanian AS, Steblevskii AV, Kolosov EN. Phase diagram of the As-S system. Inorganic Materials. 2007;43(2):95–104.

[17] Gavezzotti A, Demartin F, Castellano C, Campostrini I. Polymorphism of As_4S_3 (tris-(μ_2-sulfido)-tetra-arsenic): accurate structure refinement on natural α- and β-dimorphites and inferred room temperature thermodynamic properties. Physics and Chemistry of Minerals. 2013;40:175–182.

[18] Roberts AC, Ansell HG, Bonardi M. Pararealgar, a new polymorph of AsS, from British Columbia. Canadian Mineralogist. 1980;18:525–527.

[19] Bonazzi P, Bindi L, Popova V, Pratesi G, Menchetti S. Alacranite, As_8S_9: structural study of the holotype and re-assignment of the original chemical formula. American Mineralogist. 2003;88:1796–1800.

[20] Campostrini I, Demartin F, Russo M. A new ammonium arsenite chloride from the Solfatara di Pozzuoli, Napoli, Italy. Rendiconit della Società Geologica (Statements of the Italian Geological Society). 2014;31(Suppl.1):309.

[21] Whitfield HJ. Crystal structure of the β-form of tetra-arsenic trisulphide. Journal of the Chemical Society Dalton Transactions. 1973;17:1737–1738.

[22] Demartin F, Gramaccioli CM, Campostrini I, Orlandi P. Demicheleite, BiSBr, a new mineral from La Fossa crater, Vulcano, Aeolian Islands, Italy. American Mineralogist. 2008;93:1603–1607.

[23] Demartin F, Gramaccioli CM, Campostrini I. Demicheleite-(Cl), BiSCl, a new mineral from La Fossa crater, Vulcano, Aeolian Islands, Italy. American Mineralogist. 2009;94:1045–1048.

[24] Demartin F, Gramaccioli CM, Campostrini I. Demicheleite-(I), BiS(I,Br,Cl), a new mineral from La Fossa crater, Vulcano, Aeolian Islands, Italy. Mineralogical Magazine. 2010;74(1):141–145.

[25] Henley RW, Mavrogenes J, Tanner D. Sulfosalt melts and heavy metal (As-Sb-Bi-Sn-Pb-Tl) fractionation during volcanic gas expansion: the El Indio (Chile) paleo-fumarole. Geofluids. 2012;12:199–215.

[26] Pinto D, Balić-Žunić T, Garavelli A, Makovicky E, Vurro F. Comparative crystal-structure study of Ag-free lillianite and galenobismutite from Vulcano, Aeolian Islands, Italy. The Canadian Mineralogist. 2006;44:159–175.

[27] Borodaev YS, Garavelli A, Garbarino C, Grillo SM, Mozgova NN, Organova NI et al. Rare sulfosalts from Vulcano, Aeolian Islands, Italy. III. Wittite and cannizzarite. The Canadian Mineralogist. 2000;38:23–34.

[28] Vurro F, Garavelli A, Garbardino C, Moëlo Y, Borodaev YS. Rare sulfosalts from Vulcano,Aeolian Islands, Italy. ll. Mozgovaite, $PbBi_4(S,Se)_7$, a new mineral species. The Canadian Mineralogist. 1999;37:1499–1506.

[29] Borodaev YS, Garavelli A, Garbardino C, Grillo SM, Mozgova NN, Uspenskaya TY, et al. Rare sulfosalts from Vulcano, Aeolian Islands, Italy. IV. Lillianite. The Canadian Mineralogist. 2001;39:1383–1396.

[30] Moëlo Y, Makovicky E, Mozgova NN, Jambor JL, Cook N, Pring A, et al. Sulfosalt systematics: a review. Report of the sulpfosalt sub-committee of the IMA Commission on Ore Mineralogy. European Journal of Mineralogy. 2008;20:7–46.

[31] Borodaev YS, Garavelli A, Garbarino C, Grillo SM, Mozgova NN, Paar WH, et al. Rare sulfosalts from Vulcano, Aeolian Islands, Italy. V. Selenian Heyrovskýite. The Canadian Mineralogist. 2003;41:429–440.

[32] Borodaev YS, Garavelli A, Kuzmina O, Mozgova NN, Organova NI, Trubkin NV, et al. Rare sulfosalts from Vulcano, Aeolian Islands, Italy. I. Se-bearing kirkiite, $Pb_{10}(Bi,As)_6(S,Se)_{19}$. The Canadian Mineralogist. 1998;36:1105–1114.

[33] Garavelli A, Mozgova NN, Orlandi P, Bonaccorsi E, Pinto D, Moëlo Y, et al. Rare sulfosalts from Vulcano, Aeolian Islands, Italy. VI. Vurroite, $Pb_{20}Sn_2(Bi,As)_{22}S_{54}Cl_6$, a new mineral species. The Canadian Mineralogist. 2005;43:703–711.

[34] Pinto D, Bonaccorsi E, Balić-Žunić T, Makovicky E. The crystal structure of vurroite, $Pb_{20}Sn_2(Bi,As)_{22}S_{54}Cl_6$: OD-character, polytypism, twinning, and modular description. American Mineralogist. 2008;93:713–727.

[35] Métrich N, Wallace PJ. Volatile abundances in basaltic magmas and their degassing paths tracked by melt inclusions. Reviews in Mineralogy and Geochemistry. 2008;69:363–402.

[36] Ustunisik G, Nekvasil H, Lindsley DH, McCubbin FM. Degassing pathways of Cl^-, F^-, H^-, and S-bearing magmas near the lunar surface: implications for the composition and Cl isotopic values of lunar apatite. American Mineralogist. 2015;100:1717–1727.

[37] Villemant B, Boudon G. H_2O and halogen (F, Cl, Br) behaviour during shallow magma degassing processes. Earth and Planetary Science Letters. 1999;168: 271–286.

[38] Barone G, Mazzoleni P, Priolo G. Catalogo delle mineralizzazioni secondarie riscontrate all'interno di alcune grotte vulcaniche etnee (A catalogue of the secondary mineralizations in some Etnean volcanic caves). In: Proceedings of XXII Congresso Nazionale di Speleologia "Condividere i dati", Sessione Documentatione – a1; 30 May – 2 June 2015; Pertosa-Auletta (SA). pp. 99–109.

[39] Oskarsson N. The chemistry of Icelandic lava incrustations and the latest stages of degassing. Journal of Volcanology and Geothermal Research. 1981;10:93–111.

[40] Coradossi N, Garavelli A, Salamida M, Vurro F. Evolution of Br/Cl ratios in fumarolic salammoniac from Vulcano (Aeolian Islands, Italy). Bulletin of Volcanology. 1996;58:310–316.

[41] Roberts AC, Venance KE, Seward TM, Grice JD, Paar WH. Lafossaite, a new mineral from the La Fossa Crater, Vulcano, Italy. Mineralogical Record. 2006;37:165–168.

[42] Campostrini I, Russo M. Lafossaite e dimorphite: due nuove specie per il Vesuvio (Lafossaite and dimorphite: two new mineral species from Vesuvius). Micro. 2012;3/2012:136–141.

[43] Palache C, Berman H, Frondel C. The System of Mineralogy of James Dwight Dana and Edward Salisbury Dana Yale University 1837–1892, Volume II. 7th ed. New York: John Wiley and Sons, Inc.; 1951. 1124 p.

[44] Cruciani G, Orlandi P, Pasero M, Russo M. First Italian occurrence of cumengeite from Vesuvius: crystal-structure refinement and revision of the chemical formula. Mineralogical Magazine. 2005;69(6):1037–1045.

[45] Jacobsen MJ, Balić-Žunić T, Mitolo D, Katerinopoulou A, Garavelli A, Jakobsson SP. Oskarssonite, AlF_3, a new fumarolic mineral from Eldfell volcano, Heimaey, Iceland. Mineralogical Magazine. 2014;78(1):215–222.

[46] Rosenberg PE. Stability relations of aluminium hydroxyl-fluoride hydrate, a ralstonite-like mineral, in the system AlF_3-Al_2O_3-H_2O-HF. The Canadian Mineralogist. 2006;44;125–134.

[47] Demartin F, Campostrini I, Castellano C, Russo M. Parascandolaite, $KMgF_3$, a new perovskite-type fluoride from Vesuvius. Physics and Chemistry of Minerals. 2014;41:403–407.

[48] Russo M, Campostrini I. Ammineite, matlockite and post 1944 eruption fumarolic minerals at Vesuvius. Plinius. 2011;37:312.

[49] Garavelli A, Vurro F. Barberiite, NH_4BF_4, a new mineral from Vulcano, Aeolian Islands, Italy. American Mineralogist. 1994;79:381–384.

[50] Bernauer F. Eine Gearksutit-Lagerstätte auf der Insel Vulcano (A gearksutite-deposit on the island Vulcano). Zeitschrift der Deutschen Gesellschaft für Geowissenschaften (Journal of the German Geoscientific Society). 1941;93:65–80.

[51] Balić-Žunić T, Garavelli A, Mitolo D, Acquafredda P, Leonardsen E. Jakobssonite, $CaAlF_5$, a new mineral from fumaroles at the Eldfell and Hekla volcanoes, Iceland. Mineralogical Magazine. 2012;76(3):751–760.

[52] Mitolo D, Garavelli A, Balić-Žunić T, Acquafredda P, Jakobsson SP. Leonardsenite, $MgAlF_5(H_2O)_2$, a new mineral species from Eldfell volcano, Heimaey Island, Iceland. The Canadian Mineralogist. 2013;51:377–386.

[53] Courbion G, Ferrey G. $Na_2Ca_3Al_2F_{14}$: a new example of a structure with "independent F" – a new method of comparison between fluorides and oxides of different formula. Journal of Solid State Chemistry. 1988;76:426–431.

[54] Demartin F, Gramaccioli CM, Campostrini I. Thermessaite, $K_2[AlF_3|SO_4]$, a new ino-aluminofluoride-sulfate from La Fossa crater, Vulcano, Aeolian Islands, Italy. The Canadian Mineralogist. 2008;46:693–700.

[55] Garavelli A, Mitolo D, Pinto D. Thermessaite-(NH_4), IMA 2011-077. CNMNC Newsletter No. 12, February 2012; page 152; Mineralogical Magazine. 2012;76:151–155.

[56] Effenberger H, Kluger F. Ralstonit: ein Beitrag zur Kenntnis von Zusammensetzung und Kristallstruktur (Ralstonite: a contribution to the knowledge of its composition and crystal structure). Neues Jahrbuch fuer Mineralogie. Monatshefte. 1984;1984:97–108.

[57] de Pape R, Ferey G. A new form of FeF_3 with the pyrochlore structure: soft chemistry synthesis, crystal structure, thermal transitions and structural correlations with the other forms of FeF_3. Materials Research Bulletin. 1986;21(8):971–978.

[58] Ferey G, Leblanc M, de Pape R. Crystal structure of the ordered pyrochlore $NH_4Fe^{(II)}Fe^{(III)}F_6$ structural correlations with $Fe_2F_5(H_2O)_2$ and its dehydration product $Fe_2F_5H_2O$. Journal of Solid State Chemistry. 1981;40:1–7.

[59] Vergasova LP, Semyonova TF, Epifanova VB, Filatov SK, Chubarov VM. Meniaylovite, $Ca_4AlSi(SO_4)F_{13}\cdot 12H_2O$, a new mineral of volcanic exhalations. Vulkanologiya i Seismologiya (Volcanology and Seismology). 2004;2:3–5.

[60] Demartin F, Gramaccioli CM, Campostrini I, Castellano C. Cossaite, $(Mg_{0.5},\square)Al_6(SO_4)_6(HSO_4)F_6\cdot 36H_2O$, a new mineral from La Fossa crater, Vulcano, Aeolian Islands, Italy. Mineralogical Magazine. 2011;75(6):2847–2855.

[61] Cossa A. Sulla hieratite, nuova specie mineralogica (About hieratite, new mineral species). Transunti dell'Accademia dei Lincei (Summaries of the Lincei Academy). 1881–1882;3(6):141–142.

[62] Gramaccioli CM, Campostrini I. Demartinite, a new polymorph of K_2SiF_6 from La Fossa crater, Vulcano, Aeolian Islands, Italy. The Canadian Mineralogist. 2007;45:1275–1280.

[63] Garavelli A, Balić-Žunić T, Mitolo D, Acquafredda P, Leonadsen E, Jakobsson SP. Heklaite, $KNaSiF_6$, a new fumarolic mineral from Hekla volcano, Iceland. Mineralogical Magazine. 2010;74:147–157.

[64] Demartin F, Gramaccioli CM, Campostrini I. Knasibfite, $K_3Na_4[SiF_6]_3[BF_4]$, a new hexafluorosilicate-tetrafluoroborate from La Fossa crater, Vulcano, Aeolian Islands, Italy. The Canadian Mineralogist. 2008;46:447–453.

[65] Russo M, Campostrini I, Demartin F. Fumarolic minerals after the 1944 Vesuvius eruption. In: Abstracts, Congresso SGI-SIMP; 10–12 September 2014; Milan. Rendiconti Societa Geologica Italiana. 2014;31(Suppl. 1):315.

[66] Mitolo D, Pinto D, Garavelli A, Bindi L, Vurro F. The role of the minor substitutions in the crystal structure of natural challacolloite, KPb_2Cl_5, and hephaistosite, $TlPb_2Cl_5$, from Vulcano (Aeolian Archipelago, Italy). Mineralogy and Petrology. 2009;96:121–128.

[67] Campostrini I, Demartin F, Gramaccioli CM. Hephaistosite, $TlPb_2Cl_5$, a new mineral species from La Fossa crater, Vulcano, Aeolian Islands, Italy. The Canadian Mineralogist. 2008;46:701–708.

[68] Demartin F, Gramaccioli CM, Campostrini I. Brontesite, $(NH_4)_3PbCl_5$, a new product of fumarolic activity from La Fossa Crater, Vulcano, Aeolian Islands, Italy. The Canadian Mineralogist. 2009;47:1237–1243.

[69] Demartin F, Campostrini I, Gramaccioli CM. Panichiite, natural ammonium hexachlorostannate(IV), $(NH_4)_2SnCl_6$, from La Fossa Crater, Vulcano, Aeolian Islands, Italy. The Canadian Mineralogist. 2009;47:367–372.

[70] Demartin F, Gramaccioli CM, Campostrini I. Steropesite, Tl_3BiCl_6, a new thallium bismuth chloride from La Fossa Crater, Vulcano, Aeolian Islands, Italy. The Canadian Mineralogist. 2009;47:373–380.

[71] Demartin F, Campostrini I, Castellano C, Gramaccioli CM. Argesite, $(NH_4)_7Bi_3Cl_{16}$, a new mineral from La Fossa Crater, Vulcano, Aeolian Islands, Italy: A first example of the $[Bi_2Cl_{10}]^{4-}$ anion. American Mineralogist. 2012;97:1446–1451.

[72] Parascandola A. I minerali di Vesuvio nella eruzione del marzo 1944 e quelli formati durante l'attuale periodo di riposo (Vesuviam minerals from the March 1944 eruption, and those formed during the present quiescent period). Bollettino della Società Geologica Italiana (Bulletin of the Italian Geological Society). 1952;70:523–526.

[73] Kyriakopoulos K, Kanakis Sotiriou R, Stamatakis M. The authigenic minerals formed from volcanic emanations at Soussaki, West Attica peninsula, Greece. The Canadian Mineralogist. 1990;28:363–368.

[74] Demartin F, Gramaccioli CM, Campostrini I. Clinometaborite, natural beta-metaboric acid from La Fossa Crater, Vulcano, Aeolian Islands, Italy. The Canadian Mineralogist. 2011;49:1273–1279.

[75] Murashko MN, Pekov IV, Krivovichev SV, Chernyateva AP, Yapaskurt VO, Zadov AE, et al. Steklite, $KAl(SO_4)_2$: a finding at the Tolbachik Volcano, Kamchatka, Russia, validating its status as a mineral species and crystal structure. Geology of Ore Deposits. 2013;55(7):594–600.

[76] Demartin F, Gramaccioli CM, Campostrini I. Pyracmonite, $(NH_4)_3Fe(SO_4)_3$, a new ammonium iron sulfate from La Fossa Crater, Vulcano, Aeolian Islands, Italy. The Canadian Mineralogist. 2010;48:307–313.

[77] Demartin F, Campostrini I, Castellano C. Aluminopyracmonite, IMA 2012-075. CNMNC Newsletter No. 15, February 2013, page 9. Mineralogical Magazine, 2013;77:1–12.

[78] Balić-Žunić T, Garavelli A, Acquafredda P, Leonardsen E, Jakobsson SP. Eldfellite, $NaFe(SO_4)_2$, a new fumarolic mineral from Eldfell volcano, Iceland. Mineralogical Magazine. 2009;73:51–57.

[79] Campostrini I, Demartin F, Gramaccioli CM. Vulcano: ein aussergewohnlicher Fundpunkt von neuen und seltenen Mineralien. MineralienWelt. 2010;21(3):40–57.

[80] Burke EAJ. A mass discreditation of GQN minerals. The Canadian Mineralogist. 2006;44:1557–1560.

[81] Mofaddel N, Bouaziz R, Mayer M. Le polymorphisme du sulfate de sodium anhydre et les phases intermediaires, glaserite et aphtitalite, dans le binaire Na_2SO_4-K_2SO_4. Thermochimica Acta. 1991;185:141–153.

[82] Okada K, Ossaka J. Structures of potassium sodium sulphate and tripotassium sodium disulphate. Acta Crystallographica. 1980;B36:919–921.

[83] Garavelli A, Grasso MF, Vurro F. Sublimates and fumarolic incrustations at Mt. Etna from 1993 to 1996. Acta Vulcanologica. 1997;9:87–89.

[84] Demartin F, Castellano C, Campostrini I. Therasiaite, $(NH_4)_3KNa_2Fe^{2+}Fe^{3+}(SO_4)_3Cl_5$, a new sulphate chloride from La Fossa Crater, Vulcano, Aeolian Islands, Italy. Mineralogical Magazine. 2014;78(1):203–213.

[85] Mees F, Hatertand F, Rowe R. Omongwaite, $Na_2Ca_5(SO_4)_6 \cdot 3H_2O$, a new mineral from recent salt lake deposits, Namibia. Mineralogical Magazine. 2008;72(6):1307–1318.

[86] Autenrieth H, Braune G. Ein neues Salzmineral, seine Eigenschaften, sein Auftreten und seine Existenzbedingungen im System der Salze ozeanischer Salzablagerungen (A new salt mineral, its properties, its occurence and the conditions for its existence in the system of salts of oceanic salt deposits). Naturwissenschaften. 1958;45(15):362–363.

[87] Demartin F, Campostrini I, Castellano C, Gramaccioli CM, Russo M. D'ansite-(Mn), $Na_{21}Mn^{2+}(SO_4)_{10}Cl_3$ and d'ansite-(Fe), $Na_{21}Fe^{2+}(SO_4)_{10}Cl_3$, two new minerals from volcanic fumaroles. Mineralogical Magazine. 2012;76(7):2773–2783.

[88] Demartin F, Gramaccioli CM, Campostrini I, Pilati T. Aiolosite, $Na_2(Na_2Bi)(SO_4)_3Cl$, a new sulfate isotypic to apatite from La Fossa crater, Vulcano, Aeolian Islands, Italy. American Mineralogist. 2010;95:382–385.

[89] Demartin F, Gramaccioli CM, Campostrini I. Adranosite, $(NH_4)_4NaAl_2(SO_4)_4Cl(OH)_2$, a new ammonium sulfate chloride from La Fossa crater, Vulcano, Aeolian Islands, Italy. The Canadian Mineralogist. 2010;48:315–321.

[90] Mitolo D, Demartin F, Garavelli A, Campostrini I, Pinto D, Gramaccioli, et al. Adranosite-(Fe), $(NH_4)_4NaFe_2(SO_4)_4Cl(OH)_2$, a new ammonium sulfate chloride from La Fossa crater, Vulcano, Aeolian Islands, Italy. The Canadian Mineralogist. 2013;51:57–66.

[91] Garavelli A, Pinto D, Mitolo D, Bindi L. Leguernite, $Bi_{12.67}O_{14}(SO_4)_5$, a new Bi oxysulfate from the fumarole deposit of La Fossa crater, Vulcano, Aeolian Islands, Italy. Mineralogical Magazine. 2014;78:1629–1645.

[92] Demartin F, Castellano C, Gramaccioli CM. Campostriniite, $(Bi^{3+},Na)_3(NH_4,K)_2Na_2(SO_4)_6 \cdot H_2O$, a new sulfate isostructural with görgeyite, from La

Fossa Crater, Vulcano, Aeolian Islands, Italy. Mineralogical Magazine. 2015;79(4):1007–1018.

[93] Vergouwen L. Eugsterite, a new salt mineral. American Mineralogist. 1981;66:632–636.

[94] Slyusareva MN. Hydroglauberite, a new mineral of the hydrous sulphate group. American Mineralogist. 1970;55:321.

[95] Alpers CN, Jambor JL, Nordstrom DK. Sulfate minerals – crystallography, geochemistry, and environmental significance. Reviews in Mineralogy and Geochemistry. 2000;40:22.

[96] Sarp H, Deferne J. Chessexite, a new mineral. American Mineralogist. 1984;69:406.

[97] Thordarson Th, Höskuldsson Á. Postglacial volcanism in Iceland. Jökull. 2008;58:197–228.

[98] Harðarson BS, Fitton JG, Hjartarson Á. Tertiary volcanism in Iceland. Jökull. 2008;58:161–178.

[99] Jakobsson S, Jónasson K, Sigurðsson IA. The three igneous rock series in Iceland. Jökull. 2008;58:117–138.

[100] Þórarinsson S, Einarsson Þ, Sigvaldason GE, Elísson G. The submarine eruption off the Vestman Islands 1963–1964. A preliminary report. Bulletin of Volcanology. 1964;27:435–445.

[101] Þórarinsson S. Sitt af hverju um Surtseyjargosið. (Some facts about the Surtsey eruption.) Náttúrufræðingurinn (Naturalist). 1966;35:153–181.

[102] Þórarinsson S. Síðustu þættir Eyjaelda. (The last phases of the Surtsey eruption.) Náttúrufræðingurinn (Naturalist). 1969;38:113–135.

[103] Jakobsson SP, Jónsson SS, Leonardsen ES. Encrustations from lava caves in Surtsey, Iceland. A preliminary report. Surtsey Research Progress Report. 1992;10:73–78.

[104] Þórarinsson S, Steinþórsson S, Einarsson Þ, Kristmannsdóttir H Óskarsson N. The eruption on Heimaey, Iceland. Nature. 1973;241:372–375.

[105] Jakobsson SP, Pedersen AK, Rønsbo JG, Larsen LM. Petrology of mugearite-hawaiite: early extrusives in the 1973 Heimaey eruption, Iceland. Lithos. 1973;6:203–214.

[106] Sigurðsson O. Jarðeldar á Heimaey. (Eruption in Heimaey.) Týli. 1974;4:5–26.

[107] Sigmundsson G, Hreinsdóttir S, Hooper A, Árnadóttir T, Pedersen R, Roberts MJ, et al. Intrusion triggering of the 2010 Eyjafjallajökull eruption. Nature. 2010;468:426–430.

[108] Sigmarsson O, Vlastelic I, Andreasen R, Bindeman I, Devidal J-L, Moune S, et al. Remobilization of silicic intrusion by mafic magmas during the 2010 Eyjafjallajökull eruption. Solid Earth. 2011;2:271–281.

[109] Jónasson K, Jakobsson SP. Encrustations from the 2010 Fimmvörðuháls eruption. In: 30th Nordic Geological Winter Meeting: Programme and Abstracts, 9–12. January 2012. Reykjavík: Geoscience Society of Iceland; 2012.

[110] Þórarinsson S. Course of events. In: The Eruption of Hekla 1947–1948. Vísindafélag Ísl. 1976;4(1): 1–33.

[111] Schythe JC. Hekla og dens sidste udbrud, den 2den September 1845 (Hekla and its latest eruption, the 2nd September 1845). Kjöbenhavn: Bianco Lunos Bogtrykkeri; 1847. 154 p.

[112] Guðmundsson Á., Óskarsson N, Grönvold K, Sæmundsson K, Sigurðsson O, Stefánsson R, et al. The 1991 eruption of Hekla, Iceland. Bulletin of Volcanology. 1992;54:238–246.

[113] Sigvaldason GE. Some geochemical and hydrothermal aspects of the 1961 Askja eruption. Beiträge zur Mineralogie und Petrographie (Contributions to Mineralogy and Petrography). 1964;10:263–274.

[114] Þórarinsson S. Sigvaldason GE. The eruption in Askja, 1961. A preliminary report. American Journal of Science. 1962;260:641–651.

[115] Þórarinsson S. Askja on fire. Reykjavík: Almenna bókafélagið; 1963. 54 p.

[116] Björnsson A. Dynamics of crustal rifting in NE Iceland. Journal of Geophysical Research. 1985;90:10151–10162.

[117] Piochi M, Pappalardo L, De Astis G. Geochemical and isotopical variations within the Campanian Comagmatic Province: implications on magma source composition. Annals of Geophysics. 2004;47(4):1485–1499.

[118] Piochi M, Mormone A, Balassone G, Strauss H, Troise C, De Natale G. Native sulfur, sulfates and sulfides from the active Campi Flegrei volcano (southern Italy): genetic environments and degassing dynamics revealed by mineralogy and isotope geochemistry. Journal of Volcanology and Geothermal Research. 2015;304:180–193.

[119] Sgavetti M, Pompilio L, Roveri M, Manzi V, Valentino GM, Lugli S, et al. Two geologic systems providing terrestrial analogues for the exploration of sulfate deposits on Mars: initial spectral characterization. Planetary and Space Science. 2009;57:614–627.

[120] Russo M. Realgar e pararealgar della solfatara di Pozzuoli (Napoli) (Realgar and pararealgar from the Pozzuoli solfatara (Neaples). Micro. 2004;2004:25–28.

[121] Rolandi G, Paone A, Di Lascio M, Stefani G. The 79 AD eruption of Somma: the relationship between the date of the eruption and the southeast tephra dispersion. Journal of Volcanology and Geothermal Research. 2007;169:87–98.

[122] Chiodini G, Marini L, Russo M. Geochemical evidence for the existence of high-temperature hydrothermal brines at Vesuvio volcano, Italy. Geochimica et Cosmochimica Acta. 2001;65:2129–2147.

[123] Caliro S, Chiodini G, Avino R, Minopoli C, Bocchino B. Long time-series of chemical and isotopic compositions of Vesuvius fumaroles: evidence for deep and shallow processes. Annals of Geophysics. 2011;54:137–149.

[124] De Astis G, Lucchi F, Dellino P, La Volpe L, Tranne C A, Frezzotti ML, et al. Geology, volcanic history and petrology of Vulcano (central Aeolian archipelago). Geological Society, London, Memoirs. 2013;37:281–349.

[125] Paonita A, Favara R, Nuccio PM, Sortino F. Genesis of fumarolic emissions as inferred by isotope mass balances: CO_2 and water at Vulcano Island, Italy. Geochimica et Cosmochimica Acta. 2002;66:759–772.

[126] Capasso G, D'Alessandro W, Favara R, Inguaggiato S, Parello F. Interaction between the deep fluids and the shallow groundwaters on Vulcano Island (Italy). Journal of Volcanology and Geothermal Research. 2001;108:187–198.

[127] Coltelli M, Del Carlo P, Vezzoli L. The discovery of a Plinian basaltic eruption of Roman age at Etna volcano, Italy. Geology. 1998;26:1095–1098.

[128] Neri M, Acocella V, Behncke B. The role of the Pernicana fault system in the spreading of Mt. Etna (Italy) during the 2002–2003 eruption. Bulletin of Volcanology. 2004;66:417–430.

[129] Branca S, Del Carlo P. Eruptions of Mt. Etna during the past 3200 years: a revised compilation integrating the historical and stratigraphical records. In: Bonaccorso A, Calvari S, Coltelli M, Negro CD, Falsaperla S, editors. Mt. Etna: Volcano Laboratory. Washington: American Geophysical Union; 2004. pp. 1–22.

[130] Liotta M, Paonita A, Caracausi A, Martelli M, Rizzo A, Favara R. Hydrothermal processes governing the geochemistry of the crater fumaroles at Mount Etna volcano (Italy). Chemical Geology. 2010;278:92–104.

[131] Papazachos BC, Comninakis PE. Geophysical and tectonic features of the Aegean Arc. Journal of Geophysical Research. 1971;76:8517–8533.

[132] Nicholls JA. Petrology of Santorini volcano, cyclades, Greece. Journal of Petrology. 1971;12(1):67–119.

[133] Keller J. Mediterranean island arcs. In: Thorpe RS, editor. Andesites. New York: Wiley; 1982. pp. 307–325.

[134] Fytikas M, Innocenti F, Manetti P, Mazzuoli R, Peccerillo A, Villari L. Tertiary to quaternary evolution of volcanism in the Aegean region. Geological Society London Special Publications. 1984;17(1):687–699.

[135] Fytikas M, Innocenti F, Kolios N, Manetti P, Mazzuoli R, Poli G, et al. Volcanology and petrology of volcanic products from the island of Milos and neighbouring islets. Journal of Volcanology and Geothermal Research. 1986;28:297–317.

[136] Pe-Piper G, Piper DJW. Volcanism at subduction zones; Aegean area. Bulletin of the Geological Society of Greece. 1972; 9:113–144.

[137] Pe-Piper G, Hatzipanagiotou K. The Pliocene volcanic rocks of Crommyonia, western Greece and their implications for the early evolution of the South Aegean arc. Geological Magazine. 1997;134:55–66.

[138] Liakopoulos A, Katerinopoulos A, Markopoulos T, Bouleègue, J. A mineralogical petrographic and geochemical study of samples from wells in the geothermal field of Milos Island (Greece). Geothermics. 1991;20(4):237–256.

[139] Tarney J, Barr SR, Mitropoulos P, Sideris K, Katerinopoulos A, Stouraiti H. Santorini: geochemical constraints on magmas sources and eruption mechanisms. The European Laboratory Volcanoes. 1996;EUR18161EN:89–112.

[140] Bagnato E, Tamburello G, Aiuppa A, Sprovieri M, Vougioukalakis GE, Parks M. Mercury emissions from soils and fumaroles of Nea Kameni volcanic centre, Santorini (Greece). Geochemical Journal. 2013;47:437–450.

[141] Chiodini G, Cioni R, Leonis C, Marini L, Raco B. Fluid geochemistry of Nisyros Island, Dodecanese, Greece. Journal of Volcanology and Geothermal Research. 1993;56:95–112.

[142] D'Alessandro W, Brusca L, Kyriakopoulos K, Michas G, Papadakis G. Hydrogen sulphide as a natural air contaminant in volcanic/geothermal areas: the case of Soussaki, Corinthia (Greece). Environmental Geology. 2009;57(8):1723–1728.

[143] D'Alessandro W, Brusca L, Martelli M, Rizzo A, Kyriakopoulos K. Geochemical characterization of natural gas manifestations in Greece. Bulletin of the Geological Society of Greece. 2010;43(5):2327–2337.

[144] Kiyosu Y, Kurahashi M. Origin of sulfur species in acid sulfate-chloride thermal waters, northeastern Japan. Geochimica et Cosmochimica Acta. 1983;47:1237–1245.